An Energy-based Control Architecture for Shared Autonomy

Federico Benzi, *Student Member, IEEE*, Federica Ferraguti, *Member, IEEE*, Giuseppe Riggio, and Cristian Secchi, *Senior Member, IEEE*

***Abstract*—In robotic applications where the autonomy is shared between the human and the robot, the autonomous behavior of the robotic system is determined considering mainly the task to be executed and the data collected from the environment using, e.g., formal methods and machine learning techniques. Nevertheless, it is important to correctly translate high-level decision into low-level control inputs in order to avoid an unstable behavior due to a naive implementation of the autonomy. In this paper, we propose an energy-based architecture for shared autonomy that allows to reproduce as closely as possible the desired behavior while ensuring a robust stability of the robotic system. The proposed architecture is experimentally validated in two application scenarios: shared control of a multi-robot system and variable admittance control in human robot collaboration.**

***Index Terms*—Physical Human-Robot Interaction, Multi-robot Systems, Optimization and Optimal Control, Human-Centered Robotics.**

I. Introduction

THE shared autonomy paradigm allows to effectively combine irreplaceable human capabilities, such as cognition and expertise, with peculiar robot skills, such as a wider workspace and precision. Nowadays shared autonomy is playing a more and more significant role in many application areas, exploiting one or more robots. In surgical robotics shared autonomy is exploited for implementing semi-autonomous robotics surgery [1], [2]. In industrial applications shared autonomy allows to improve the execution of several tasks [3], [4]. In physical human robot collaboration the autonomy of the robot can be used, e.g., for stabilizing the interaction [5], for improving the job quality [6]–[8], for role adaptation [9]. When the human is managing multiple robots, shared autonomy is almost mandatory and a lot of work has been done for interacting with a group of robots [10]–[12].

In shared autonomy, the behavior of the robotic system depends both on the human input and on the autonomy allocated to the robotic system itself. The input of the human, provided either remotely (e.g. by teleoperation) or locally (e.g. by physical interaction) is blended with the autonomy of the robot. Such a control structure allows the human and the robot to take care of the most cognitive intensive tasks and of the lower level tasks respectively. In order to make the human aware of the behavior of the robotic system, a feedback signal is generated and sent to the user. Typically, haptic signals are employed (see e.g. [11], [13] for further details). For the execution of a simple task in a static environment, a single kind of autonomous behavior, which can be implemented through a predefined control architecture, is sufficient (see e.g. [12]). Nevertheless, shared autonomy systems have often to deal with complex tasks where the robotic system needs to interact with a variable and dynamic environment. In these cases, a high-level autonomy allocation strategy that takes care of adapting the autonomous behavior of the robot and of sending the corresponding control commands, is necessary.

The impressive advances in machine/deep learning, in formal methods for task description and the availability of huge datasets have provided robots with an unprecedented awareness of the environment and of the tasks they have to execute. This gave birth to several high-level decisions making strategies that provide control commands for a very flexible and seamless adaptation of the level of autonomy and for a contextual assistance to the human (see e.g. [14]–[16]).

Nevertheless, such high-level flexible commands have to be correctly translated into low-level control actions that deterministically ensure stability and safety for the human and for the robot (see [13] for a discussion on this issue). Thus, it is crucial to design a control architecture that allows to implement the high flexibility achievable by high-level decision makers into a corresponding safe and stable behavior. This problem is recently receiving a lot of attention by the robotics community and several control strategies for harnessing harmful behaviors have been proposed.

Control barrier functions have been used for generating a safe approximation of a desired input generated by a Reinforcement Learning strategy [17], [18]. Energy-based control strategies have been used for ensuring the stability when the interaction dynamics changes in human robot collaboration [5], model predictive control has also been used for dealing with possibly destabilizing effects due to learned policies [2], [19].

Nevertheless, at the best of the Authors' knowledge, a general architecture suitable for embedding high-level policies in a shared control setting in order to optimally implement the desired behavior while ensuring stability guarantees is not available yet. Furthermore, when the robot has to interact with the environment, whose position and dynamics may not be perfectly known, the problem of guaranteeing a stable interaction becomes even harder. In fact, it is necessary to guarantee robust stability, i.e. a stable behavior of the robot both in free motion and during the contact with an unknown physical system and during the transition between free motion

F. Benzi, F. Ferraguti and C. Secchi are with the Department of Engineering Sciences and Methods (DISMI), University of Modena and Reggio Emilia, Italy {federico.benzi, federica.ferraguti,cristian.secchi}@unimore.it
G. Riggio is with System Logistics s.p.a., Fiorano Modenese, Italy

and contact (and viceversa).

Thus, the key features of a control architecture for shared autonomy are robust stability, for enabling a stable behavior both in contact/non contact scenarios, and flexibility, for maximally enabling the reactivity of the high-level decision strategies.

Passivity based control has been widely exploited for achieving a robustly stable interaction with an unknown environment. The two main reasons behind the success of passivity in robotics are physical equivalence and modularity. In fact, in most of the cases, both the controller and the controlled system are equivalent to a physical system (e.g. mass-spring-damper in impedance/admittance control [20], distributed mass-spring system in communication channels with wave variables [21], nonlinear spring-damper in multi-robot control [22]). This makes the resulting behavior easier to understand and the implementation (e.g. tuning) more intuitive. If a controlled system is passive, it is characterized by a stable behavior. Furthermore, because of modularity, coupling a passive system with another passive system (e.g. the environment) leads to a coupled system that is still passive and, therefore, stable [23]. Finally, it has been recently shown that passivity is a necessary and sufficient condition for achieving a robust stability [24].

Thus, passivity guarantees both robust stability and a stable interaction with any, possibly unknown, passive environment. Passivity based control has been successfully exploited in bilateral teleoperation [21], [25], [26], in multi-robot systems control [11], [12], [27], in collaborative robotics [5], [28], [29] and in many other fields of robotics.

Nevertheless, traditional passivity-based control cannot achieve a good level of flexibility and implement an effective shared autonomy architecture. In fact, selecting a specific passive dynamics may lead to severe limitations on the kind of behavior that can be achieved. In teleoperation it is often useful to change the stiffness of the coupling in order to adapt the interaction to different users/environments (see e.g. [30]). In human-robot collaboration impedance adaptation is important for optimizing the interaction [31], [32]. In multi-robot scenarios it is important that some agents implement a reactive behaviour (i.e. due to active perception constraints [33] or to coverage needs [34]) and a fixed coupling with the other robots may prevent the implementation of a proper reaction and it can lead to a trade-off suboptimal behavior.

Energy tanks [5], [35], [36] have been introduced for disembodying passivity-based control from specific physical dynamics. They are used for storing the energy dissipated by the system, in order to later re-employ it for reproducing desired behaviors in a passive way. Using energy tanks it is possible to achieve an high flexibility while preserving passivity and, therefore, robust stability.

In this paper we propose a tank based control architecture for shared autonomy that exploits passivity for ensuring a robustly stable behavior and that leverages energy tanks for ensuring a maximally flexible passive behavior. We will not focus on the design of the strategy, often task dependent, that needs to be implemented by the high-level decision maker for generating the desired behavior but rather on the best robustly stable implementation of a desired high-level behavior.

The proposed system takes a control input that comes from a high-level decision maker that may not take into account stability issues. Thus, the proposed architecture derives the closest input to be applied to the system for guaranteeing a passive, and consequently robustly stable, behavior.

We will prove that if the desired behavior is passive it can always be perfectly implemented using the proposed architecture and, therefore, that standard passivity based control is a particular case of the proposed architecture for shared control. Furthermore, we will show how to implement the proposed architecture over a delayed communication channel. The tank based architecture will be illustrated and experimentally validated on two meaningful use cases: a physical human robot interaction scenario, where the robot needs to adapt to the human for guaranteeing a stable behavior, and a multi-robot shared control case, where the human teleoperates a fleet of robots that need to keep a cohesive behavior. Thus, thanks to the proposed architecture, it will be possible to achieve a shared autonomy system that can flexibly and seamlessly adapt the autonomy of the robotic system while preserving a robustly stable behavior.

Some preliminary results of this paper have been presented in [37] and in [38]. In [37] energy tanks have been used for passively implementing an interconnection among passive agents, but the concept of optimal passive implementation was not present in the paper. In [38], the optimized use of the energy in the tank is introduced for a physical human-robot interaction context but shared autonomy systems are not considered. The main contributions of this paper are:

- A general control architecture for shared autonomy that enables the flexibility necessary when the human is sharing the authority with a robot and that guarantees a robustly stable interconnection.
- A framework for extending the proposed architecture over delayed communication channels.
- A shared control strategy for a collaborative robotic system and for a multi-robot system exploiting the proposed architecture.
- An experimental validation of the proposed architecture on a collaborative scenario and on teleoperation of a multi-robot system scenario.

This paper is organized as follows: in Sec. II the related works are analyzed and the novelty of the architecture proposed in the paper is highlighted. In Sec. III the problem addressed in this paper is stated and in Sec. IV the concept of modulated tank is introduced. In Sec. V the main energetic infrastructure for flexible and robustly stable interactive control is presented and in Sec. VI a strategy for making the controllers robust with respect to communication delay is illustrated. In Sec. VII the overall energy-based control architecture for shared autonomy is derived and in Sec. VIII it is specialized for implementing a variable admittance control. In Sec. IX the proposed architecture is experimentally validated on a multi-robot scenario and on a physical human-robot collaborative system. Finally, in Sec. X conclusions are drawn.

II. Related Works

Passivity-based control has been successfully exploited in the context of shared autonomy systems.

In many applications, it is possible to reproduce a desired authority by forcing the robotic system to mimic a passive physical dynamics. This is the case of dynamic virtual fixtures [39], where visco-elastic dynamics, the fixtures, are used for guiding the user or for keeping it away from forbidden region. Because of the intuitive design and the robust stability due to passivity, virtual fixtures are widely used in shared control applications [40]–[42]. When the human is interacting with a multi-robot system, some authority for reproducing the desired group behavior (e.g. cohesiveness) is often delegated to the robot. These fleet behaviors are often obtained by linking the robots with nonlinear springs and dampers in order to reproduce a passive and stable dynamics [12], [22], [43]. In physical human-robot interactions impedance/admittance control [20] is used for defining the way the robot needs to react to the interaction with the human by reproducing a desired physical dynamics (e.g. mass-spring-damper) and this represents a form or authority allocated to the robot. Several works addressed the use of optimization techniques in passivity-based control. Optimization problems have been designed for finding passive stabilizing inputs [44], [45] or for tuning passivity-based controllers [46].

These approaches can reproduce a desired authority in a robustly stable way but they are designed for reproducing a specific target behavior. In a shared authority scenario, the target behavior can be highly variable and designing a passivity based control capable of reproducing a wide set of very diverse behaviors may lead, if any, to a very complex controller. Thus, standard passivity based controllers are not flexible enough to dynamically reproduce a highly variable command coming from the implemented authority (e.g. add/remove virtual fixtures, change the stiffness of the coupling among some robots in a swarm, change the inertia in an impedance controller).

Interpreting passivity as a byproduct of a physical embodiment, i.e. a specific physical dynamics, leads to over-conservative choices (e.g. do not change the physical dynamics) for preserving passivity and, therefore, to a lack of flexibility. Actually, passivity is an energetic property and a specific (physical) dynamics is just an instantiation of a specific energetic behavior. By taking this point of view, it is possible to implement a much more flexible passivity-based control.

The time domain passivity approach (TDPA) [47] does not pose limits on the dynamic behavior to reproduce. It monitors the energy flowing through the system and it activates a variable damper for dissipating the excess of energy due to non passive behaviors. TDPA has been successfully exploited in shared authority applications [48], [49]. TDPA is a reactive approach and, therefore, the passifying damping action can lead to passive behaviors that are quite different from the desired ones. The Passive Setpoint Modulation (PSPM) [50] guarantees passivity by modulating the signal to be sent to the robot controlled by a PD and it has been successfully applied to shared authority applications [51]. PSPM flexibly handles the passivation but the necessary presence of the PD introduces a distortion on the reproduced dynamic behavior.

Energy tanks [35] can be used to separate the passivity problem from the desired target behavior, acting as a sort of passivity filter, allowing to passively reproduce any desired control dynamics (e.g. time-varying, discontinuous), according to a task-dependent heuristic, while keeping the control architecture very simple.

Energy tanks have been successfully exploited for achieving high-performance teleoperation systems by splitting the passivity constraint from the desired performance [35], [36], [52], [53], in multi-robot systems for passively implementing behaviors that would have been impossible to achieve by reproducing a specific physical dynamics [11], [27], [28], in force control for overcoming the limitation of traditional algorithms [38], [54]–[57], in human-robot collaboration for flexibly adapting the interaction [5], [58], [59] and in teach by demonstration for enabling a passive stiffness variation [60], [61].

The current energy tank-based approaches have two main limitations. First, since the tank stores mainly the energy dissipated, it is necessary to know the model of the system the tank is interconnected to. Second, there is the need of a strategy for passively approximating non-passive actions without depleting the tank. There is no clear guideline on the definition of such a strategy and many task dependent heuristics have been proposed in the literature. These task-dependent heuristics can lead to a sub-optimal passive approximation of the desired control action and, consequently, to sub-optimal performance.

The control architecture proposed in this paper allows to reproduce any passive dynamics and, therefore, it can replicate all the passivity-based approaches for implementing a specific target behavior.

Furthermore, the proposed control strategy represents a significant evolution on energy tank-based control, as it overcomes the current limitations of standard energy tank-based controllers. In fact, using the proposed architecture, the energy tank stores the energy that can be exploited for passively reproducing a desired input without requiring the model of the system it is connected to. This overcomes the first limitation of current energy tank-based control, making the proposed architecture more robust with respect to the state of the art. Additionally, given a desired input to implement using the energy in the tank, its best passive approximation can be found by solving a convex optimization problem. This eliminates the need of finding heuristics for building a passive approximation of a non-passive input and it overcomes the second limitation of current energy tank-based controllers.

The proposed control architecture allows to achieve the best passive approximation of a desired control input by solving an optimization problem. Unlike TDPA and PSPM, it does not resort to ancillary dynamics for passivation. In fact, while extra passivating dynamics allow to achieve in a physically intuitive way a passive approximation of the desired behavior, they also introduce spurious dynamic effects (due to their dynamic nature) on the passivated output and they do not usually allow to obtain the best passive approximation. Energy tanks

are free from extra passivating dynamics, but they still fail to implement an optimal approximation of a desired control action due to the second limitation mentioned above.

The problem of optimally passifying a desired dynamics has been recently addressed in [62], where a passivity constraint is embedded in an optimization problem for generating a passive control input. The passivity constraint is computed by keeping track of the power available at each instant of time, leading to an overly conservative approach. Thanks to the energy tank, the architecture proposed in the paper formulates the passivity constraint in the optimization problem exploiting the energy available up to the current instant of time. This makes the solution that can be found less conservative and it allows to find better passive approximation.

In summary, the paper proposes a novel energy tank-based architecture that can generate the best passive approximation of a desired dynamics, without the need of knowing the model of the system and of defining an heuristic for the use of energy. Furthermore, no ancillary dynamics are needed and, therefore, no spurious effects are introduced. This allows to generate a variable authority in a robustly stable and flexible way using a very simple control architecture.

Thus, when integrated in a shared autonomy system, the proposed architecture allows to dynamically filter the commands of the autonomy allocation strategy in order to optimally reproduce the desired autonomy in a robustly stable way.

III. Problem Statement

We consider a shared autonomy architecture, where a robotic system, formed either by a single robot (e.g. a robotic arm) or by several robots (e.g. a multi-robot system), is controlled partly by the human operator and partly by an autonomy allocation strategy. The human operator can interact with the robotic system either directly or by means of a local robotic device through teleoperation. The autonomy allocation strategy can generate commands that may produce unstable behaviors. We will build a control architecture for passively reproducing the commands requested by the autonomy allocation strategy in order to achieve an optimal robustly stable behavior of the robotic system. We will develop our architecture for the general case in which the human remotely controls a group of robots through a local device by teleoperation and where an autonomy allocation strategy decides the autonomous behavior of all the robots. We will then show how the proposed architecture can be reduced for a simpler case where the human directly interacts with the robot (i.e. no local device, no teleoperation dynamics) and where the robotic system consists of a single robot.

More formally, consider a robotic system made up of N robots modeled by the following Euler-Lagrange equations:

$$\mathbf{M}_i(\mathbf{x}_i)\ddot{\mathbf{x}}_i + \mathbf{C}_i(\mathbf{x}_i,\dot{\mathbf{x}}_i)\dot{\mathbf{x}}_i + \mathbf{D}_i(\mathbf{x}_i)\dot{\mathbf{x}}_i = -\mathbf{F}_{C_i} + \mathbf{F}_{R_i} + \mathbf{F}_{E_i} \quad i = 1,\dots,N, \tag{1}$$

where $\mathbf{x}_i, \dot{\mathbf{x}}_i \in \mathbb{R}^n$ are the pose and the velocity of the robot and we set $\mathbf{v}_i = \dot{\mathbf{x}}_i$. $\mathbf{M}_i > 0$ and $\mathbf{D}_i \geq 0$ are the positive definite inertia matrix and the positive semi-definite damping matrix, respectively, while $\mathbf{C}_i(\mathbf{x}_i,\dot{\mathbf{x}}_i)$ represents the Coriolis terms. The force $\mathbf{F}_{R_i} \in \mathbb{R}^n$ is the input for connecting the robot with an external device that can be used by the human to control the robot itself, $\mathbf{F}_{E_i} \in \mathbb{R}^n$ is the force due to the interaction with the environment, while $\mathbf{F}_{C_i} \in \mathbb{R}^n$ is the control input. More specifically, $\mathbf{F}_{C_i} = \mathbf{F}_{cont_i} + \mathbf{F}_{int_i} \in \mathbb{R}^n$ where $\mathbf{F}_{cont_i}$ is the control input for shaping the i^{th} robot behavior and $\mathbf{F}_{int_i} = \sum_{j=1}^{N} \mathbf{F}_{int_{ij}}$ is the force due to the dynamic interconnection with the other robots.

Based on the knowledge of the task and on the processing of the external data (e.g. semantic perception, real time data from the user), without necessarily considering low level stability issues, an autonomy allocation strategy dynamically provides to each robot the desired behavior and the desired interconnection with the other robots, i.e. a desired value $\mathbf{F}^d_{C_i}(t) = \mathbf{F}^d_{cont_i}(t) + \mathbf{F}^d_{int_i}(t) \in \mathbb{R}^n$. For example, the autonomy allocation strategy can decide to stiffen the interactive behavior of an admittance/impedance controlled robot in certain working phases or it can decide to produce a novel cohesive behavior of a multi-robot system by changing the dynamic interconnection among the robots.

The human operator can interact with the robotic system by means of a local device coupled to the robotic system. In the following, we will use the term *local device* to indicate the device at the operator side and *remote robot* to define the robot which interacts with the environment. The local device is described by

$$\mathbf{M}_l(\mathbf{x}_l)\ddot{\mathbf{x}}_l + \mathbf{C}_l(\mathbf{x}_l,\dot{\mathbf{x}}_l)\dot{\mathbf{x}}_l + \mathbf{D}_l(\mathbf{x}_l)\dot{\mathbf{x}}_l = \mathbf{F}_H + \mathbf{F}_l, \tag{2}$$

where $\mathbf{x}_l, \dot{\mathbf{x}}_l \in \mathbb{R}^n$ are the pose and the velocity of the robot. $\mathbf{M}_l > 0$ and $\mathbf{D}_l \geq 0$ are the positive definite inertia matrix and the positive semi-definite damping matrix respectively while $\mathbf{C}_l(\mathbf{x}_l,\dot{\mathbf{x}}_l)$ represents the Coriolis terms. The forces $\mathbf{F}_H, \mathbf{F}_l \in \mathbb{R}^n$ are the forces exerted by the human and the input force connecting the local device to the robotic system. In order to make the notation more compact, we introduce the following notation

$$\mathbf{F}_R = \begin{pmatrix} \mathbf{F}_{R_1} \\ \vdots \\ \mathbf{F}_{R_N} \end{pmatrix} \quad \mathbf{F}_E = \begin{pmatrix} \mathbf{F}_{E_1} \\ \vdots \\ \mathbf{F}_{E_N} \end{pmatrix} \quad \mathbf{F}_C = \begin{pmatrix} \mathbf{F}_{C_1} \\ \vdots \\ \mathbf{F}_{C_N} \end{pmatrix}$$
$$\mathbf{F}^d_C = \begin{pmatrix} \mathbf{F}^d_{C_1} \\ \vdots \\ \mathbf{F}^d_{C_N} \end{pmatrix} \quad \mathbf{v} = \begin{pmatrix} \dot{\mathbf{x}}_1 \\ \vdots \\ \dot{\mathbf{x}}_N \end{pmatrix}. \tag{3}$$

Furthermore, we will set $\mathbf{v}_l = \dot{\mathbf{x}}_l$.

We aim at designing a control architecture for optimally reproducing the behavior determined by the autonomy allocation strategy while guaranteeing stable behavior. In other words, the control strategy has to guarantee:

- **Robust Stability**, i.e. the robotic system has to behave in a stable way both in free motion and during the interaction with the environment. We will achieve this result by ensuring the passivity of the overall controlled system.
- **Flexibility**, i.e. to control the robotic system in such a way to follow as closely as possible the desired inputs

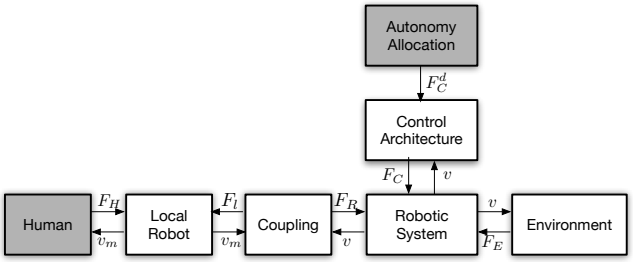

Fig. 1. The considered shared autonomy scenario. The robotic system can be controlled by the human, through a local device coupled with the robots, and by the autonomy allocation strategy. The desired control input produced by the autonomy block is elaborated by the control architecture whose aim is to produce the desired behavior as faithfully as possible while guaranteeing robots stability.

provided by the autonomy allocation strategy. This will be achieved by exploiting energy tanks and by optimizing the control input based on the available energy.

An illustration of the problem addressed in the paper is provided in Fig. 1. The shared autonomy system consists of a robotic system that can be controlled by the human and by an high-level autonomy allocation strategy. The human commands are transmitted by means of a local device properly coupled with the robots. The commands of the autonomy allocation strategy are transmitted to the robots through the control architecture whose aim is to reproduce $\mathbf{F}_C^d$ as faithfully as possible while preserving a stable behavior of the overall system.

In this way, the autonomy allocation module can be maximally flexible in defining the desired control inputs, i.e. disregarding motion/contact stability constraints, and the proposed architecture will minimally perturb the desired input for generating a maximally flexible and stable behavior of the system.

IV. Passivity and Modulated Energy Tanks

In this section we introduce the concepts of passivity and of modulated energy tank. We will provide the definition of passivity and the main results used in the paper and we will show how to use modulation for reproducing any desired behavior exploiting the energy stored in the tank. For further information, the reader is addressed to [38].

Consider the following nonlinear system

$$\Sigma = \begin{cases} \dot{\boldsymbol{\chi}}(t) = \phi(\boldsymbol{\chi}(t)) + \eta(\boldsymbol{\chi}(t))\boldsymbol{\mu} \\ \boldsymbol{\lambda}(t) = \psi(\boldsymbol{\chi}), \end{cases} \tag{4}$$

where $\chi \in \mathbb{R}^p$ and $\mu, \lambda \in \mathbb{R}^r$ are the state, the input and the output of the system. The vector field $\phi : \mathbb{R}^p \to \mathbb{R}^p$ represents the internal dynamics of the system, $\eta : \mathbb{R}^p \to \mathbb{R}^{p\times r}$ is a state dependent input matrix and $\psi : \mathbb{R}^p \to \mathbb{R}^r$ is the output map.

Definition 1. *[63] The system Σ is passive with respect to the pair $(\boldsymbol{\mu}, \boldsymbol{\lambda})$ if there is a function of the state, called storage function, $V : \mathbb{R}^p \to \mathbb{R}^+$ such that the following balance holds for all $t > 0$:*

$$\int_0^t \boldsymbol{\mu}^T(\tau)\boldsymbol{\lambda}(\tau)d\tau \geq V(\boldsymbol{\chi}(t)) - V(\boldsymbol{\chi}(0)) \geq -V(\boldsymbol{\chi}(0)). \tag{5}$$

The pair $(\boldsymbol{\mu}, \boldsymbol{\lambda})$ is called *power port*, or simply port, of the system. The product $\boldsymbol{\mu}^T\boldsymbol{\lambda}$ is the (generalized) power crossing the power port.

Passive systems are characterized by a stable behavior: if left free to evolve (i.e. $\boldsymbol{\mu} = 0$) their equilibrium configurations are (locally) stable; if the input is bounded, then the output is bounded as long as the inequality in (5) is strict. More information can be found in, e.g., [63], [64].

Passivity-based control consists of designing a control strategy that makes the controlled system dynamics passive. This allows to achieve stabilization goals and to intuitively set the desired transient (see e.g. [63], [64] for more details). In robotics, passivity-based control has been successfully exploited both for stabilization purposes and for achieving desired dynamic couplings between the robots and the environments they are interacting with. Besides having proven very effective, making the dynamics of the controlled robot passive is also necessary for maintaining a stable behavior when the robot is interacting with the environment, as proven in [24].

The energy tank [35], [36] is an energy storing element represented by the following dynamics:

$$\begin{cases} \dot{x}_t = u_t \\ y_t = \frac{\partial T}{\partial x_t} = x_t, \end{cases} \tag{6}$$

where $x_t \in \mathbb{R}$ is the state of the tank and $(u_t, y_t) \in \mathbb{R} \times \mathbb{R}$ is the power port through which the tank can exchange energy with the rest of the world. The energy stored in the tank is given by

$$T(x_t) = \frac{1}{2}x_t^2 \tag{7}$$

and, combining (6) with (7), it is easy to show that

$$\dot{T} = u_t y_t. \tag{8}$$

The tank is not associated to a physical dynamics, it is just an element storing/releasing energy through its power port (u_t, y_t).

The energy stored in the tank can be used for reproducing any desired behavior for a generic input/output port $(\mathbf{u}, \mathbf{y}) \in \mathbb{R}^q \times \mathbb{R}^q$ by implementing the following modulation between (u_t, y_t) and $(\mathbf{u}, \mathbf{y})$

$$\begin{cases} u_t = \mathbf{a}^T(t)\mathbf{u} \\ \mathbf{y} = \mathbf{a}(t)y_t, \end{cases} \tag{9}$$

where $\mathbf{a}(t) \in \mathbb{R}^q$ is given by

$$\mathbf{a}(t) = \frac{\boldsymbol{\gamma}(t)}{x_t} \tag{10}$$

and $\boldsymbol{\gamma}(t) \in \mathbb{R}^q$ is the desired value for the output $\mathbf{y}(t)$. From (9) it follows that

$$\mathbf{u}^T\mathbf{y} = \mathbf{u}^T\mathbf{a}(t)y_t = u_t y_t, \tag{11}$$

that means that the power crossing $(\mathbf{u}, \mathbf{y})$ is the same as the power crossing the power port of the tank (u_t, y_t). In other words, no power is generated or dissipated by the modulation. By plugging (9) in (6) we get the modulated energy tank that is represented by

$$\begin{cases} \dot{x}_t = \mathbf{a}^T(t)\mathbf{u} \\ \mathbf{y} = \mathbf{a}(t)y_t = \boldsymbol{\gamma}(t). \end{cases} \tag{12}$$

The modulated tank (12) is endowed with a power port $(\mathbf{u}, \mathbf{y}) \in \mathbb{R}^q \times \mathbb{R}^q$ and the modulation term $\mathbf{a}(t)$ allows to exploit the energy in the tank for reproducing any desired value $\boldsymbol{\gamma}(t)$ for the output. When interconnecting a robot to the modulated energy tank, the pair $(\mathbf{u}, \mathbf{y})$ will be a force-velocity pair. In this way, thanks to the modulation, the energy in the tank is transformed into mechanical energy.

Because of the singularity of (10), the desired port-behavior cannot be implemented when $x_t = 0$. This mathematical condition has a deep physical implication. In fact, from (7) it follows that having $x_t = 0$ means that no more energy is stored in the tank and, therefore, nothing can be implemented. Thus, in order to avoid singularities in (12), it is necessary to initialize x_t in such a way that $T(x_t(0)) \geq \varepsilon$ and to guarantee that $T(x_t(t)) \geq \varepsilon$, where $\varepsilon > 0$ is a lower bound for the energy stored in the tank. If the energy requested for implementing a desired port behavior exceeds the amount of energy stored in the tank, only an approximation of the desired output can be implemented. Several heuristics for approximating the desired output are available in the literature [11], [36], [54], [65].

It is possible to prove that the modulated tank (12) implements a passive exchange of energy as long as the tank is not empty.

Proposition 1. *If $T(x_t(0)) \geq \varepsilon$ and $T(x_t(t)) > \varepsilon$ for all $t > 0$, then the modulated tank* (12) *is passive independently of the desired value $\boldsymbol{\gamma}(t)$.*

Proof. From (12) and (7) we have that

$$\dot{T} = \frac{\partial T}{\partial x_t}\dot{x_t} = x_t \mathbf{a}^T(t)\mathbf{u} = \mathbf{y}^T\mathbf{u}, \tag{13}$$

where the last equality can be obtained by (9) considering the definition of y_t in (6).

The balance in (13) leads to

$$\int_0^t \mathbf{u}^T(\tau)\mathbf{y}(\tau)d\tau = T(x_t(t)) - T(x_t(0)) \geq -T(x_t(0)), \tag{14}$$

which proves the passivity of (12). □

Thus, as long as the tank is not empty, it is possible to passively implement any desired port behavior using the energy stored in the tank.

If the energy initially stored in the tank is sufficient, then it is possible to reproduce any passive port-behavior using (12) without ever depleting the tank and, therefore, avoiding singularities in (10). A similar result has been proven for energy tanks and single port systems interconnected to passive plants in [66]. In this paper, we extend this result to general multi-port passive dynamics and modulated energy tanks.

Proposition 2. *Let $\mathcal{S}$ be a system passive with respect to M ports $(\mathbf{u}_{\sigma_i}(t), \mathbf{y}_{\sigma_i}(t)) \in \mathbb{R}^q \times \mathbb{R}^q$ for $i = 1, \ldots, M$ using the non negative storage function $S(t)$. If $x_t(0)$ is chosen such that $T(x_t(0)) \geq S(0) + \varepsilon$, then the ports behavior can be reproduced by the modulated tank* (12) *without depleting the tank.*

Proof. Define $\mathbf{u}_\sigma, \mathbf{y}_\sigma \in \mathbb{R}^{qM}$ as

$$\mathbf{u}_\sigma = \begin{pmatrix} \mathbf{u}_{\sigma_1} \\ \vdots \\ \mathbf{u}_{\sigma_M} \end{pmatrix} \quad \mathbf{y}_\sigma = \begin{pmatrix} \mathbf{y}_{\sigma_1} \\ \vdots \\ \mathbf{y}_{\sigma_M} \end{pmatrix}. \tag{15}$$

The port-behavior of $\mathcal{S}$ can be reproduced by feeding (12) with $\mathbf{u} = \mathbf{u}_\sigma$ and by setting $\boldsymbol{\gamma}(t) = \mathbf{y}_\sigma$ in (10).

Since $\mathcal{S}$ is passive with respect to $(\mathbf{u}_{\sigma_i}(t), \mathbf{y}_{\sigma_i}(t))$ for $i = 1, \ldots, M$ we have that

$$\sum_{i=1}^{M} \int_0^t \mathbf{u}_{\sigma_i}^T(\tau)\mathbf{y}_{\sigma_i}(\tau)d\tau = \int_0^t \mathbf{u}_\sigma^T(\tau)\mathbf{y}_\sigma(\tau)d\tau \geq S(t) - S(0). \tag{16}$$

From (14) we have that

$$\int_0^t \mathbf{u}_\sigma^T(\tau)\mathbf{y}_\sigma(\tau)d\tau = T(x_t(t)) - T(x_t(0)). \tag{17}$$

Thus, from (16) and (17) we have that:

$$T(x_t(t)) \geq S(t) - S(0) + T(x_t(0)) \geq -S(0) + T(x_t(0)), \tag{18}$$

where the last inequality derives from the non negativity of the storage function $S(t)$. Since $T(x_t(0)) > S(0) + \varepsilon$ we have that

$$T(x_t(t)) \geq \varepsilon \quad \forall t > 0, \tag{19}$$

which proves the statement. □

This result shows that passivity can be completely disembodied from any physical dynamics and that it depends only on the way energy is used. In fact, the port-behavior of any passive system can be implemented through the energy flow of the tank, a generic energy storing element.

From Proposition 1 we have that any dynamics that does not deplete the tank is passive. On the other hand, from Proposition 2 we have that, as long as some initial conditions are satisfied, any passive dynamics can be implemented without depleting the tank. Thus, we can conclude that a dynamic system is passive if and only if it can be perfectly reproduced without depleting the tank. In other words, the tank represents an abstraction of all passive dynamics.

Remark 1. *If too much energy is stored in the tank, it may happen that practically unstable behaviors can be implemented, as shown in [50]. This problem can be solved by saturating the energy tank as shown in [5], [36]. In order to keep the presentation simple, we do not consider the saturation in this paper. All the results keep on holding also for saturated tanks.*

V. Modulated Tank based Control

In this section, we exploit the concept of modulated energy tank for building a control strategy for implementing the desired control action $\mathbf{F}_C^d$ for the robotic system defined in Sec. III while ensuring passivity (i.e. robust stability) and flexibility of the behavior of the robots. This control strategy will be the main ingredient of the energy-based architecture for shared autonomy.

The modulated tank-based control is illustrated in Fig. 2. The robotic system is made up of the N robots described by

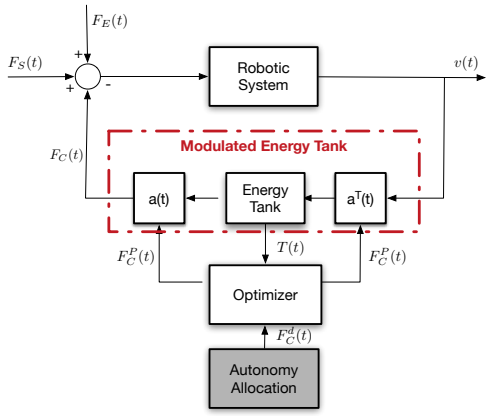

Fig. 2. The modulated tank-based control scheme. The input and the output of the modulated tank are the velocities of the robots $\mathbf{v}(t)$ and the control forces to be applied $\mathbf{F}_C(t)$, respectively. The autonomy allocation block generates the desired control input $\mathbf{F}_C^d(t)$ to be sent to the optimization block. The optimizer computes the closest passive approximation $\mathbf{F}_C^P(t)$ of the desired behaviour $\mathbf{F}_C^d(t)$ by solving (24) via a convex optimization solver.

(1) and it can be modeled as a single Euler-Lagrange model given by

$$\mathbf{M}(\mathbf{x})\ddot{\mathbf{x}} + \mathbf{C}(\mathbf{x},\dot{\mathbf{x}})\dot{\mathbf{x}} + \mathbf{D}(\mathbf{x})\dot{\mathbf{x}} = -\mathbf{F}_C + \mathbf{F}_R + \mathbf{F}_E, \quad (20)$$

where $\mathbf{x} = (\mathbf{x}_1^T, \dots, \mathbf{x}_N^T)^T$ and $\dot{\mathbf{x}} = (\dot{\mathbf{x}}_1^T, \dots, \dot{\mathbf{x}}_N^T)^T =: \mathbf{v}$. The inertia, Coriolis and damping matrices are block diagonal matrices given by $\mathbf{M}(\mathbf{x}) = diag(\mathbf{M}_1(\mathbf{x}_1), \dots, \mathbf{M}_N(\mathbf{x}_N))$, $\mathbf{C}(\mathbf{x},\dot{\mathbf{x}}) = diag(\mathbf{C}(\mathbf{x}_1,\dot{\mathbf{x}}_1), \dots, \mathbf{C}(\mathbf{x}_N,\dot{\mathbf{x}}_N))$ and $\mathbf{D}(\mathbf{x}) = diag(\mathbf{D}_1(\mathbf{x}_1), \dots, \mathbf{D}_N(\mathbf{x}_N))$ respectively. The terms $\mathbf{F}_C, \mathbf{F}_R, \mathbf{F}_E \in \mathbb{R}^{nN}$ represent the control inputs, the inputs due to the interaction with the local device and the force due to the environment, respectively, and they are defined in (3).

The total kinetic energy of the robotic system is given by

$$\mathcal{K} = \sum_{i=1}^{N} \frac{1}{2}\dot{\mathbf{x}}_i^T \mathbf{M}_i(\mathbf{x}_i)\dot{\mathbf{x}}_i = \frac{1}{2}\dot{\mathbf{x}}^T \mathbf{M}(\mathbf{x})\dot{\mathbf{x}} \quad (21)$$

and it is well known, see e.g. [23], that (20) is passive with respect to the pair $(-\mathbf{F}_C + \mathbf{F}_R + \mathbf{F}_E, \mathbf{v})$ using as a storage function the kinetic energy $\mathcal{K}$ and, consequently, the following power balance holds:

$$\int_0^t \left((-\mathbf{F}_C(\tau) + \mathbf{F}_R(\tau) + \mathbf{F}_E(\tau))^T \mathbf{v}(\tau)\right) d\tau \geq \mathcal{K}(t) - \mathcal{K}(0). \quad (22)$$

A modulated energy tank (12) endowed with a power port $(\mathbf{u},\mathbf{y}) \in \mathbb{R}^{nN} \times \mathbb{R}^{nN}$ is interconnected to the robotic system by means of the following interconnection

$$\begin{cases} \mathbf{u} = \mathbf{v} \\ \mathbf{y} = \boldsymbol{\gamma}(t) = \mathbf{F}_C^P(t). \end{cases} \quad (23)$$

The input and the output of the modulated tank are the velocities of the robots and the control forces to be applied. At each instant of time the autonomy allocation strategy generates a desired control input $\mathbf{F}_C^d(t)$ which is sent to an optimization block. The optimizer, considering the energy available in the tank and the desired behavior, computes the closest passive approximation $\mathbf{F}_C^P(t)$ of the desired behavior $\mathbf{F}_C^d(t)$. The output of the optimizer is then used for modulating the way the energy of the tank is exploited by setting $\boldsymbol{\gamma}(t) = \mathbf{F}_C^P(t)$ in (10).

The role of the optimization in the control architecture is crucial since applying $\mathbf{F}_C^d(t)$ directly to the modulation of (12) can lead to a loss of passivity. In fact, if $\mathbf{F}_C^d(t)$ corresponds to a non passive behavior, its implementation can lead to a depletion of the tank and, consequently, the results of Proposition 1 are not valid anymore and a singularity appears in (10). This problem can be faced by considering the tank as a sort of filter, i.e. by preventing the implementation of a control action that requires more energy than the one stored in the tank, as done e.g. in [35], [54], [67]. Nevertheless, this simple strategy can lead to a big loss in terms of efficiency since the implemented dynamics can significantly differ from the desired one.

In this paper, we propose to consider passivity as a constraint to satisfy during the implementation of the desired control action. This allows to recast the problem of passively reproducing the desired input into an optimization problem. According to Proposition 1, it is sufficient to guarantee that $T(x_t(t)) \geq \varepsilon$ in order to ensure the passivity of (12). Thus, given a desired control input $\mathbf{F}_C^d(t)$, it is possible to find its best passive implementation $\mathbf{F}_C^P(t)$ by simply solving the following optimization problem.

$$\min_{\mathbf{F}_C^P(t)} \|\mathbf{F}_C^P(t) - \mathbf{F}_C^d(t)\|^2 \quad (24a)$$

$$T(x_t(t)) \geq \varepsilon \quad (24b)$$

Then, by setting $\boldsymbol{\gamma}(t) = \mathbf{F}_C^P(t)$ in (10) it is possible to implement the best passive approximation of the desired behavior without depleting the tank and, consequently, guarantee the passivity of the modulated tank.

In order to take (24) in a more amenable form, the passivity constraint (24b) can be reformulated in such a way that it contains the variable to optimize. Since $\mathbf{y}(t) = \boldsymbol{\gamma}(t) = \mathbf{F}_C^P(t)$ and since, from (23), $\mathbf{u}(t) = \mathbf{v}(t)$, from (14) we can rewrite (24) as:

$$\min_{\mathbf{F}_C^P(t)} \|\mathbf{F}_C^P(t) - \mathbf{F}_C^d(t)\|^2 \quad (25a)$$

$$\int_0^t \mathbf{v}^T(\tau)\mathbf{F}_C^P(\tau)d\tau \geq -T(x_t(0)) + \varepsilon \quad (25b)$$

Thus, solving online (25) it is possible to find the best passive implementation of any desired control action $\mathbf{F}_C^d(t)$. Furthermore, if the desired control action induces a passive behavior, as shown in Proposition 1, the passivity constraint (25b) is always satisfied. This means that, using the architecture represented in Fig. 2, it is possible to reproduce exactly any desired control input corresponding to a passive dynamics. If the dynamics corresponding to the desired input is not passive, its best passive approximation is implemented.

The formulation of the optimization problem in (25) may seem complicated because of the presence of an integral constraint. Nevertheless, when considering a discrete time implementation, (25b) can be rewritten as:

$$\sum_{i=0}^{k} \mathbf{v}^T(i\xi)\mathbf{F}_C^P(i\xi)\xi = \mathbf{v}^T(k\xi)\mathbf{F}_C^P(k\xi)\xi + \underbrace{\sum_{i=0}^{k-1} \mathbf{v}^T(i\xi)\mathbf{F}_C^P(i\xi)\xi}_{T(x_t((k-1)\xi))-T(x_t(0))} \geq -T(x_t(0)) + \varepsilon, \quad (26)$$

where $\xi > 0$ represents the sampling time. The term $\sum_{i=0}^{k-1} \mathbf{v}^T(i\xi)\mathbf{F}_C^P(i\xi)\xi = T(x_t((k-1)\xi)) - T(x_t(0))$ represents the amount of energy accumulated in the tank up to time $(k-1)\xi$. From (26), we can formulate the passivity constraint as:

$$\mathbf{v}^T(k\xi)\mathbf{F}_C^P(k\xi)\xi \geq \varepsilon - T(x_t((k-1)\xi)), \quad (27)$$

which clearly states that the energy for implementing the control action at the time step k must not be greater than the energy available in the tank.

Thus, (25) can be reformulated as the following convex optimization problem:

$$\min_{\mathbf{F}_C^P(k\xi)} \|\mathbf{F}_C^P(k\xi) - \mathbf{F}_C^d(k\xi)\|^2 \quad (28a)$$

$$\boldsymbol{\mathcal{A}}(k\xi)\mathbf{F}_C^P(k\xi) \geq \mathcal{B}((k-1)\xi) \quad (28b)$$

where $\boldsymbol{\mathcal{A}}(k\xi) = \xi\mathbf{v}^T(k\xi)$ and $\mathcal{B}((k-1)\xi) = \varepsilon - T(x_t((k-1)\xi)$.

The solution of the convex optimization problem in (28) is very simple and it allows to minimize the cost function (28a) subject to the constraint (28b) that guarantees that the solution does not deplete the tank. Since (28b) is a linear constraint and, by construction, $\varepsilon - T(x_t((k-1)\xi)) \leq 0$, (25) is always feasible and, in particular, $\mathbf{F}_C^P = 0$ is always an admissible solution. Because of its low complexity, (28) can be easily solved online. The CVXgen solver [68] has been adopted for the experiments and it was possible to solve the optimization problem in real-time at 500 Hz without missing a sample. Any other equivalent solver can be used. Thus, the optimization can be easily solved online by updating the passivity constraint with the information coming from the tank.

Remark 2. *Non negligible regenerative effects can appear when discretely integrating the tank dynamics at small sampling frequencies [69]. These effects can be either integrated in the passivity constraint, using the strategy proposed in [38], or avoided using a passive discrete integrator (e.g. [70]).*

It is now possible to show the following result.

Proposition 3. *Consider* (20) *interconnected to* (12) *through* (23)*, where* $\mathbf{F}_C^P(t)$ *is obtained by solving* (25)*. The controlled system is passive with respect to the pair* $(\mathbf{F}_R + \mathbf{F}_E, \mathbf{v})$.

Proof. Consider the following non negative storage function

$$\mathcal{H} = \mathcal{K} + T, \quad (29)$$

where $\mathcal{K}$ is the kinetic energy of the robots defined in (21) and T is the energy stored in the tank defined in (7). Since $\mathbf{F}_C^P(t)$ is obtained from (25), $T(x_t(t)) \geq \varepsilon$ for all $t \geq 0$. Thus, from Proposition 1, we know that the modulated tank is passive with respect to the pair $(\mathbf{u}, \mathbf{y}) = (\mathbf{u}, \mathbf{F}_C^P)$. Since (20) is passive with respect to the pair $(-\mathbf{F}_C + \mathbf{F}_R + \mathbf{F}_E, \mathbf{v})$, we can write:

$$\int_0^t \mathbf{v}^T(\tau)\left(-\mathbf{F}_C(\tau) + \mathbf{F}_R(\tau) + \mathbf{F}_E(\tau)\right)d\tau + \int_0^t \mathbf{u}^T(\tau)\mathbf{F}_C^P(\tau)d\tau \geq \mathcal{K}(t) - \mathcal{K}(0) + T(x_t(t)) - T(x_t(0)) = \mathcal{H}(t) - \mathcal{H}(0) \geq -\mathcal{H}(0). \quad (30)$$

Using (23) in (30) we get

$$\int_0^t \mathbf{v}^T(\tau)\left(\mathbf{F}_R(\tau) + \mathbf{F}_E(\tau)\right)d\tau \geq -\mathcal{H}(0), \quad (31)$$

which concludes the proof. □

Remark 3. *When the behavior to reproduce is not passive, it can happen that only a little energy is left in the tank and, consequently, that the implemented input is far from the desired one. It is possible to harvest some energy to refill the tank by adding a (variable) damper to the controlled system. In this way, some energy is extracted from the robots and stored in the tank. Several techniques for energy harvesting have been proposed in literature (see e.g. [11], [71]).*

Using the proposed architecture, it is possible to reproduce exactly the desired behavior in many cases. In fact, if the desired control input reproduces a passive behavior or if the energy in the tank is sufficient for counterbalancing the energy produced by a desired input, (25) always admits as a minimum norm solution the desired control input and, therefore, the control performance after the optimizer are exactly the desired ones. If the energy produced by the desired control input cannot be compensated by the energy stored in the tank, the solution of (25) is the best passive implementation of the desired control input, which guarantees a stable behavior but at the cost of a degradation, the smallest, of the performance.

VI. Communication Delay in Modulated Tank Based Control

The modulated tank-based control strategy proposed in Sec. V assumes a negligible communication delay among the robots. This allows multiple robots to share the same modulated energy tank and to exploit its energy for producing the local control and the interconnection inputs of all the robots.

When the number of robots increases or when the robots are deployed on a wide area, it may happen that the communication delay becomes significant and, therefore, the use of a single shared modulated energy tank as shown in Sec. V is not possible anymore. In fact, the delay prevents the agents from directly exchanging energy with a shared tank and, if not properly handled, can destroy the passivity of the energetic interconnection (see e.g. [23]).

In order to address this problem, it is convenient to endow each robot with a modulated tank and to reproduce a shared

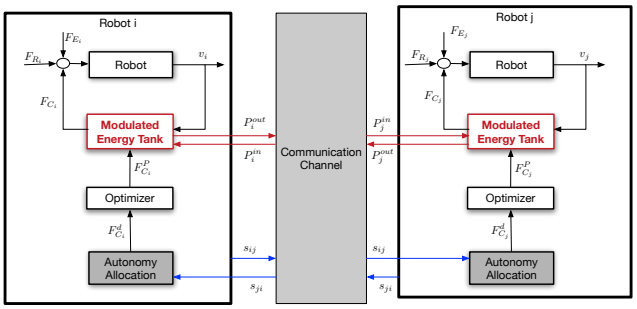

Fig. 3. The delayed modulated tank control strategy. Each tank can exchange power (red arrows) and signals (blue arrows) over a delayed communication channel. The signal s_{ij} contains any kind of information (e.g. position, velocity, force) that the robot shares with its peers and that can be used by the autonomy allocation modules for determining the desired control input.

energy tank by a proper exchange of energy over the communication channel. The delayed modulated tank control is represented in Fig. 3.

Each robot is represented by (1) and it is passive with respect to the pair $(\mathbf{v}_i, -\mathbf{F}_{C_i} + \mathbf{F}_{R_i} + \mathbf{F}_{E_i})$ with respect to the kinetic energy $\mathcal{K}_i = \frac{1}{2}\dot{\mathbf{x}}_i^T \mathbf{M}(\mathbf{x}_i)\dot{\mathbf{x}}_i$. Thus the following balance holds

$$\mathcal{K}_i(t) - \mathcal{K}_i(0) \leq \int_0^t \mathbf{v}_i^T(\tau)(-\mathbf{F}_{C_i}(\tau) + \mathbf{F}_{R_i}(\tau) + \mathbf{F}_{E_i}(\tau))d\tau. \tag{32}$$

Each robot is endowed with a local modulated tank that can exchange power through a communication channel:

$$\begin{cases} \dot{x}_{t_i} = \mathbf{a}_i^T(t)\mathbf{u}_i + \frac{1}{x_{t_i}}(P_i^{in}(t) - P_i^{out}(t)) \\ \mathbf{y}_i = \mathbf{a}_i(t) y_{t_i} = \boldsymbol{\gamma}_i(t) \end{cases} \quad i = 1, \ldots, N, \tag{33}$$

where $P_i^{in}, P_i^{out} \geq 0$ are the power received from/sent to other robots over the communication channel, respectively. The addition of the term $\frac{1}{x_{t_i}}(P_i^{in}(t) - P_i^{out}(t))$ in (33) enables storing/releasing the exchanged power into/from the tank. In fact, the energy stored in the tank is given by $T_i(x_{t_i}) = \frac{1}{2}x_{t_i}^2$ and the following power balance holds:

$$\dot{T}_i = \mathbf{y}_i^T \mathbf{u}_i + P_i^{in} - P_i^{out}, \tag{34}$$

that clearly shows that the energy stored in the tank depends also on the power flows exchanged with the communication channel.

Exploiting the information (e.g. position, velocity, force) exchanged by the robots over the communication line (indicated by the blue lines in Fig. 3), a local authority allocation module generates the desired control action $F_{C_i}^d$, i.e. the desired interconnection with the other robots and the desired local control.

The power port $(\mathbf{u}_i, \mathbf{y}_i) \in \mathbb{R}^n \times \mathbb{R}^n$ of (33) is interconnected to the i^{th} robot by

$$\begin{cases} \mathbf{u}_i(t) = \mathbf{v}_i \\ \mathbf{y}_i = \boldsymbol{\gamma}_i(t) = \mathbf{F}_{C_i}^P, \end{cases} \tag{35}$$

where $\mathbf{F}_{C_i}^P$ is the best passive approximation of $\mathbf{F}_{C_i}^d$ computed by solving a convex optimization problem that can be easily obtained starting from (34) following the steps presented in Sec. V.

Thus, each robot behaves passively and it can implement any desired local behaviour and/or interconnection with the other robots in a passive way. The desired behaviour can be computed exploiting local data or information coming from the other robots, generically denoted with s_{ij} in Fig. 3. Computing $\mathbf{F}_{C_i}^d$ using delayed information can likely lead to a non passive desired behavior but, thanks to the optimizer, only its best passive implementation is reproduced, guaranteeing flexibility and robust stability of the system.

Nevertheless, relying only on a local tank can lead to a shortage of energy and, consequently, to a decrease in performance. In fact, as shown in [71], it can happen that the overall energy stored in the tanks is sufficient for achieving good performance for all the robots but that the energy is not properly distributed (e.g. the tank of one robot has too much energy and the tank of another robot is almost empty). Allowing the modulated tanks in (33) to exchange power, it is possible to create an energetic connection through which the tanks can share energy.

Let $P_{ij}^{out}, P_{ij}^{in} \geq 0$ be the power that the tank i sends to the tank j and the power that tank i receives from tank j, where $i, j \in \{1, \ldots, N\}$. If robot i and robot j cannot communicate (e.g. occlusion, very big distance), then $P_{ij}^{out} = 0$. If the communication is possible, the amount of power sent depends on the specific power sharing strategy and it is application dependent. It can be a constant power flow $\bar{P} > 0$ as long as some energy is available in the tank, the power dissipated by the robot [36] or an amount of power due to a request from another agent [71]. We assume that $P_{ii}^{in} = P_{ii}^{out} = 0$, i.e. a tank cannot send or receive energy to/from itself.

For each modulated tank (33) we have that

$$\begin{aligned} P_i^{out} &= \textstyle\sum_{j=1}^N P_{ij}^{out} \\ P_i^{in} &= \textstyle\sum_{j=1}^N P_{ij}^{in} \end{aligned} \tag{36}$$

and, since the power is exchanged over a transmission line, we have

$$P_{ij}^{in}(t) = P_{ji}^{out}(t - \delta_{ij}), \tag{37}$$

where $\delta_{ij} \geq 0$ is the constant communication delay between robot i and robot j.

Proposition 4. *Consider N robots modeled by* (1) *interconnected to the modulated tank* (33) *by means of* (35)*. If the power inputs of* (33) *are defined as in* (36) *and if the power is exchanged over the communication channel according to* (37)*, then the overall system is passive with respect to the pair $(\mathbf{F}_R + \mathbf{F}_E, \mathbf{v})$.*

Proof. The power flowing into the communication channel is given by:

$$P_{ch}(t) = \sum_{i=1}^N P_i^{out}(t) - \sum_{i=1}^N P_i^{in}(t). \tag{38}$$

Considering (36) and (37), we can rewrite (38) as:

$$P_{ch}(t) = \sum_{i=1}^N \sum_{j=1}^N P_{ij}^{out}(t) - \sum_{i=1}^N \sum_{j=1}^N P_{ji}^{out}(t - \delta_{ij}). \tag{39}$$

By swapping the indexes in the second term, (39) can be reformulated as:

$$P_{ch}(t) = \sum_{i=1}^{N}\sum_{j=1}^{N} P_{ij}^{out}(t) - P_{ij}^{out}(t-\delta_{ij}) =: \dot{H}_{ch}(t), \quad (40)$$

whence

$$H_{ch}(t) = \sum_{i=1}^{N}\sum_{j=1}^{N} \int_{t-\delta_{ij}}^{t} P_{ij}^{out}(\tau)d\tau, \quad (41)$$

where, since $P_{ij}^{out}(t) \geq 0$, H_{ch} is the non negative storage function representing the amount of energy stored in the communication channel.

Consider now the following storage function

$$\mathcal{W} = \sum_{i=1}^{N} \mathcal{K}_i + \sum_{i=1}^{N} T_i + H_{ch}, \quad (42)$$

where $\mathcal{K}_i$ is the kinetic energy of each robot and T_i is the energy stored in (33). From (32), (34), and (40) we have that

$$\sum_{i=1}^{N} \int_0^t \mathbf{v}_i^T(\tau)[-\mathbf{F}_{C_i}(\tau) + \mathbf{F}_{R_i}(\tau) + \mathbf{F}_{E_i}(\tau)]d\tau +$$
$$+ \sum_{i=1}^{N} \int_0^t [\mathbf{v}_i^T(\tau)\mathbf{F}_{C_i}^P(\tau) + P_i^{in}(\tau) - P_i^{out}(\tau)]d\tau + \int_0^t P_{ch}(\tau)d\tau \geq$$
$$\geq \sum_{i=1}^{N} [\mathcal{K}_i(t) + T_i(t) - \mathcal{K}_i(0) - T_i(0)] + H_{ch}(t) - H_{ch}(0). \quad (43)$$

Considering (38), (35) in (43) and the non negativity of $\mathcal{K}_i$, T_i and of H_{ch} we can write:

$$\int_0^t \mathbf{v}^T(\tau)(\mathbf{F}_R(\tau) + \mathbf{F}_E(\tau))d\tau \geq$$
$$\geq \sum_{i=1}^{N} -\mathcal{K}_i(0) - T_i(0) - H_{ch}(0) = -\mathcal{W}(0), \quad (44)$$

thus concluding the proof. □

The exchange of power among the tanks allows to share the power among the robots without violating the passivity of the overall system. The communication channel acts as a storing element, where the energy traveling from one tank to the other is stored. In this way the system composed by the energy tanks and by the communication channels behaves as one distributed energy reservoir shared among all the robots.

VII. Energy-based control architecture for shared autonomy

The modulated energy tank architecture presented in the previous sections is the main ingredient for building a flexible and robustly stable energy-based control architecture for shared autonomy. The proposed architecture is represented in Fig. 4. The autonomy allocation strategy generates the desired control input $\mathbf{F}_C^d(t)$ for the robotics system. The optimizer finds the best passive approximation $\mathbf{F}_C^P(t)$ of $\mathbf{F}_C^d(t)$ by considering the energy stored in the tank $T(t)$ as shown in Sec. V. The controlled system is passive with respect to the pair $(\mathbf{F}_R + \mathbf{F}_E, \mathbf{v})$ as shown in Proposition 3. In case of a non negligible communication delay among the robots composing the robotic system, the strategy illustrated in Sec. VI can be exploited for guaranteeing a flexible and energetic consistent behavior. The overall controlled system keeps on being passive with respect to the pair $(\mathbf{F}_S + \mathbf{F}_E, \mathbf{v})$ as shown in Proposition 4.

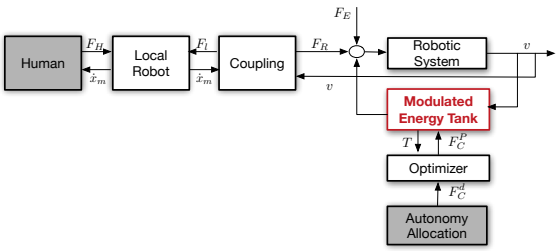

Fig. 4. The energy-based control architecture for shared autonomy. The robotic system can be controlled by the human, through the local device and by the autonomy allocation strategy. In particular, the autonomy allocation block generates the desired control input $\mathbf{F}_C^d(t)$ for the robotic system. The optimizer finds the best passive approximation $\mathbf{F}_C^P(t)$ of $\mathbf{F}_C^d(t)$ by considering the energy stored in the tank $T(t)$. Then, the modulated energy tank provides as output the control forces to be applied.

Thanks to passivity, a robustly stable behavior of the robotic system, both in free motion and while interacting with any external, passive, environment, is guaranteed. Moreover, the abstraction provided by energy tanks disembodies passivity from any specific dynamics and this brings two advantages. First, it is possible to achieve a high level of flexibility, which is of paramount importance for shared control systems. Second, independently of the nature of the desired input (e.g. discontinuous, switched, time-varying), no extra theoretical machinery (e.g. hybrid system theory) is necessary for proving the stable behavior of the robotic system. In order to preserve a robustly stable behavior when interacting with the user, we propose to couple the local device port $(\mathbf{F}_l, -\dot{\mathbf{x}}_l)$ to the controlled robotic system port $(\mathbf{F}_R, -\mathbf{v})$ using a passive coupling. This means that the following balance holds:

$$\int_0^t [-\mathbf{F}_l^T(\tau)\dot{\mathbf{x}}_l(\tau) - \mathbf{F}_R^T(\tau)\mathbf{v}(\tau)]d\tau \geq \mathcal{C}(t) - \mathcal{C}(0) \geq -\mathcal{C}(0), \quad (45)$$

where $\mathcal{C}(t)$ is a non negative storage function representing the amount of energy stored in the coupling dynamics.

The coupling can be implemented using one of the strategies available in the teleoperation literature both for non delayed communication (e.g. dampers [11], PD [72]) and for delayed communication (e.g. [26], [35], [50]) between the local and the remote robotic systems.

The passivity of the overall system follows from the passivity of the interconnection of passive systems.

Proposition 5. *The energy-based control architecture illustrated in Fig. 4 is passive with respect to the pair* $((\mathbf{F}_H^T\ \mathbf{F}_E^T)^T, (\dot{\mathbf{x}}_l^T\ \mathbf{v}^T)^T)$.

Proof. The local device is modeled as an Euler-Lagrange system (2) and, therefore (see e.g [23]), it is passive with respect to the pair $(\mathbf{F}_l + \mathbf{F}_H, \dot{\mathbf{x}}_l)$ and the following balance

holds:

$$\int_0^t [\mathbf{F}_l(\tau) + \mathbf{F}_H(\tau)]^T \dot{\mathbf{x}}_l(\tau) d\tau \geq \mathcal{K}_l(t) - \mathcal{K}_l(0) \geq -\mathcal{K}_l(0), \tag{46}$$

where $\mathcal{K}_l = \frac{1}{2}\dot{\mathbf{x}}_l^T \mathbf{M}_l(\mathbf{x}_l)\dot{\mathbf{x}}_l$ is the kinetic energy of the local device.

According to Proposition 3 or to Proposition 4 in case of communication delay, the controlled robotic system is passive with respect to the pair $(\mathbf{F}_R + \mathbf{F}_E, \mathbf{v})$ and the following balance holds

$$\int_0^t [\mathbf{F}_R(\tau) + \mathbf{F}_E(\tau)]^T \mathbf{v}(\tau) d\tau \geq \mathcal{Z}(t) - \mathcal{Z}(0) \geq -\mathcal{Z}(0), \tag{47}$$

where $\mathcal{Z} = \mathcal{H}$, as in Proposition 3, in case of no communication delay among the agents composing the robotic system, and $\mathcal{Z} = \mathcal{W}$, as in Proposition 4, in case of communication delay.

Considering the passive coupling, by summing (46), (47) and (45) we get

$$\begin{aligned} &\int_0^t [\mathbf{F}_l(\tau) + \mathbf{F}_H(\tau)]^T \dot{\mathbf{x}}_l(\tau) d\tau + \int_0^t [\mathbf{F}_R(\tau) + \mathbf{F}_E(\tau)]^T \mathbf{v}(\tau) d\tau + \\ &+ \int_0^t [-\mathbf{F}_l^T(\tau)\dot{\mathbf{x}}_l(\tau) - \mathbf{F}_R^T(\tau)\mathbf{v}(\tau)] d\tau = \int_0^T [\mathbf{F}_H^T(\tau)\dot{\mathbf{x}}_l(\tau) + \\ &+ \mathbf{F}_E^T(\tau)\mathbf{v}(\tau)] d\tau \geq -\mathcal{K}_l(0) - \mathcal{Z}(0) - \mathcal{C}(0), \end{aligned} \tag{48}$$

which proves the passivity of the system with respect to the non negative storage function $\mathcal{K}_l(t) + \mathcal{Z}(t) + \mathcal{C}(t)$. □

Remark 4. *In shared human robot collaboration, it can happen that no local device and no coupling are present, i.e. that the human is directly interacting with the robotic system. The passivity of the controlled robotic system guarantees a stable and safe human robot interaction while preserving the flexibility of the robotic system thanks to energy tanks.*

The proposed energy-based control architecture for shared autonomy allows to achieve a passive (i.e. robustly stable) and maximally flexible behavior of the robotic system both in free motion and during the interaction with the environment. The architecture is general purpose and it can be applied to many different shared control scenarios.

Remark 5. *Despite the possibility of remotely controlling the robotic system on behalf of the human, the proposed architecture significantly differs from a traditional bilateral teleoperation system. In fact, the behavior of the robotic system is only partially controlled by the user and, therefore, there may not be a position tracking between local and remote devices. Furthermore, the force fed back to the user through the coupling contains the force exchanged with the environment but also the force due to autonomy allocation and, therefore, there may not be a perfect force tracking as intended in teleoperation. Nevertheless, the force feedback is helpful to inform the user about the overall behavior of the robotic system (e.g. abrupt variations due to local autonomy decisions, possible interactions of the robotic system with the environment).*

VIII. Admittance control for Physical Human Robot Collaboration

Admittance control is a standard control strategy used for regulating the interaction of a velocity controlled robot with the environment [20]. The controlled robots mimics a desired passive behavior (e.g. mass-spring-damper) and the passivity of the admittance dynamics makes the interaction robustly stable.

Flexibility is a weak point of standard admittance control. In fact, the admittance dynamics has to be fixed and it cannot be changed online. In physical human-robot collaboration this is a strong limitation. In fact, the human can change its natural impedance during the interaction with the robot and it may be necessary to change the admittance dynamics in order to maintain a stable behavior of the coupled system [5], [31]. Furthermore, adapting online the admittance dynamics can help to improve the execution of a collaborative task [73]. Several approaches for implementing a variable admittance dynamics have been proposed in the literature (see e.g. [5], [31], [61]) but they allow to achieve a limited flexibility.

A variable admittance controlled robot physically collaborating with a human can be represented as a shared autonomy system. In fact, the human influences the behavior of the robot by directly interacting with it and the robot autonomously and dynamically adapts the admittance dynamics based on the data collected from the human and the environment and on the task knowledge, where impedance/admittance is often changed in a feedforward manner. Thus, the energy-based control architecture proposed in Sec. VII can be exploited for implementing a robustly stable and maximally flexible admittance controller. Nevertheless, the general architecture has to be adapted for considering a velocity input for the robot.

The causality of velocity controlled robot is different from the one of Euler-Lagrange systems. However, since energy tanks are "causality agnostic", the energy-based architecture can be easily adapted.

Formally, we consider a robot endowed with a high-gain low level velocity controller (e.g. a PID controller) that allows to track any desired velocity, i.e. $\mathbf{v} \approx \mathbf{v}_d$, where $\mathbf{v}, \mathbf{v}_d \in \mathbb{R}^6$ are the real and the desired velocity for the robot. The low level controller compensates the dynamics of the robot and, using admittance controller, a desired interaction dynamics is implemented. The energy-based control architecture for shared autonomy is represented in Fig. 5.

Since the human is directly interacting with the robot, the local device and the coupling block featured in the general architecture are not present anymore. The total force acting on the robot, i.e. $\mathbf{F}_H + \mathbf{F}_E$, the data collected from the human and from the environment and the knowledge of the task are sent to the autonomy allocation block that dynamically sets the best admittance dynamics and computes the corresponding desired velocity $\mathbf{v}_{adm,d}(t)$. The dynamic variation of the admittance dynamics can lead to a non passive behavior (see e.g. [5]), but the best passive approximation of the desired velocity can be

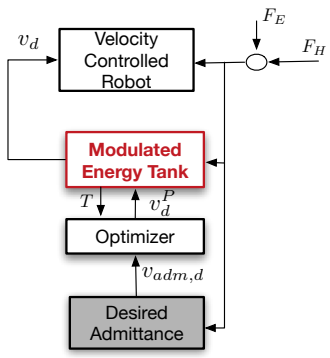

Fig. 5. The energy-based control architecture for variable admittance control. The desired admittance is computed at each time instant and provides the corresponding desired velocity $\mathbf{v}_{adm,d}(t)$ to the optimizer. The optimizer, considering the energy stored in the tank $T(t)$, computes the best approximation $\mathbf{v}_d^P(t)$ of the desired behaviour. The output $\mathbf{v}_d^P(t)$ is then used for modulating the energy flowing into/out of the energy tank and computing the desired velocity for the robot.

found by solving the following optimization problem

$$\min_{\mathbf{v}_d^P(t)} \|\mathbf{v}_d^P(t) - \mathbf{v}_{adm,d}(t)\|^2 \tag{49a}$$

$$T(x_t(t)) \geq \varepsilon \tag{49b}$$

where $T(t)$ is the energy in the tank. The modulated tank has an admittance causality and it is fed by the total force $\mathbf{F}_H + \mathbf{F}_E$ acting on the robot, it is modulated by the outcome of (49) and produces the setpoint velocity $\mathbf{v}_d$.

Following the same procedure outlined in (26) and in (27), it is possible to rewrite (49) in a convex form as:

$$\min_{\mathbf{v}_d^P(t)} \|\mathbf{v}_d^P(k\xi) - \mathbf{v}_{adm,d}(k\xi)\|^2 \tag{50a}$$

$$\boldsymbol{\mathcal{D}}(k\xi)\mathbf{v}_d^P(k\xi) \geq \mathcal{E}((k-1)\xi) \tag{50b}$$

where $\boldsymbol{\mathcal{D}}(k) = \xi(\mathbf{F}_H(k\xi) + \mathbf{F}_E(k\xi))^T$ and $\mathcal{E}(k-1) = \varepsilon - T(x_t(k-1)\xi)$. Since (49) prevents the tank from being depleted, the best passive approximation of $\mathbf{v}_{adm,d}(t)$ will always be sent as a setpoint to the robot, i.e. $\mathbf{v}_d = \mathbf{v}_d^P$. Because of Proposition 1, we have that the modulated tank is passive with respect to the pair $(\mathbf{F}_H + \mathbf{F}_E, \mathbf{v}_d)$. Since we are assuming that the low level controller implements a perfect velocity tracking, we have that $\mathbf{v} \approx \mathbf{v}_d$ and, consequently, we can say that the overall controlled robot is passive with respect to the pair $(\mathbf{F}_H + \mathbf{F}_E, \mathbf{v})$.

Thus, exploiting the proposed shared autonomy architecture, it is possible to implement a flexible admittance controller, by enabling a variable admittance dynamics, in a robustly stable way, by enforcing passivity in a minimally invasive way.

IX. Experiments

Different experiments were conducted, in order to separately test the various functionalities of the architecture.

A. Shared control of a multi-robot system

In this experiment a human operator has to drive a group of $N = 3$ mobile robots (Turtlebot3 Burger [1]) through a cluttered environment. The user commands one robot of the fleet, the leader, through a local haptic device (Force Dimension Omega6 [2]). The experimental setup is illustrated in Fig. 6.

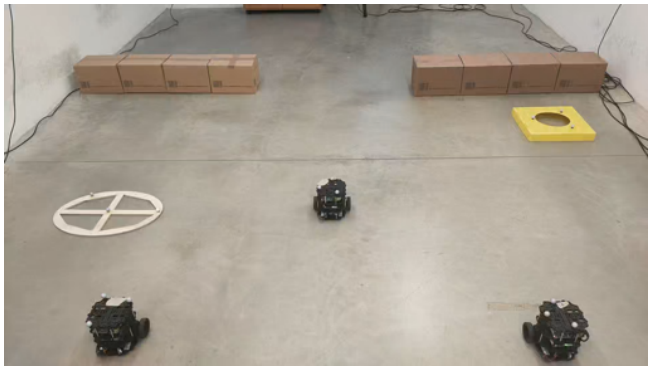

Fig. 6. Experimental setup utilized for the shared control of a multi-robot system. There are two obstacles, that the robots need to avoid, and a bottleneck the robots need to pass through.

Each mobile robot is modeled as an Euler-Lagrange system in (1). The group of robots is endowed with an autonomy allocation module that, given the positions and the velocities of the robots and the map of the environment, generates a proper cohesive behavior for the fleet. In particular, when navigating in free space, the robots should have a high relative distance in order to better cover the area; when the group has to pass through a narrow passage, a cohesive behavior with small local distances is preferred in order to facilitate the navigation.

The desired cohesive behavior can be achieved by requiring the following time-varying spring-damper coupling among the agents:

$$\mathbf{F}^d_{int_{ij}} = K_P(\mathbf{x}_{ji} - \bar{\mathbf{x}}^d_{ji}(t)) + K_D\dot{\mathbf{x}}_{ij} \quad i,j = 1,\dots,3,\ i \neq j, \tag{51}$$

where K_P and K_D are positive definite gain matrices representing stiffness and damping terms, $\mathbf{x}_{ji} = \mathbf{x}_i - \mathbf{x}_j \in \mathbb{R}^3$ is the relative position of the agents and $\bar{\mathbf{x}}^d_{ji}(t) \in \mathbb{R}^3$ is the rest length of the springs, representing the desired relative position of the robots.

The spring-damper coupling allows to achieve a cohesive behavior of the fleet. This can be tuned by adapting online $\bar{\mathbf{x}}^d_{ji}(t)$.

As shown in [23], this kind of behavior is non-passive and might introduce instabilities in the system. By exploiting the architecture in Fig. 4, it is possible to reproduce the best passive approximation $\mathbf{F}^P_C$ of the desired control input (51).

The autonomy allocation module does not implement other control inputs besides the inter-agent interconnection, implying that $\mathbf{F}^d_{C_i} = \mathbf{F}^d_{int_i} = \sum_{j=1}^N \mathbf{F}^d_{int_{ij}}$, for $i = 1,\dots,3$.

Each robot is capable of locally detecting obstacles in its surroundings and avoiding them by means of a potential repulsive field, resulting in the following interaction force with the environment:

$$\mathbf{F}_{E_i} = -\nabla U_{r_i}, \tag{52}$$

[1] https://www.turtlebot.com

[2] https://www.forcedimension.com/products/omega

in which U_{r_i} is the repulsive potential defined as

$$U_{r_i} = \sum_{k=1}^{Q} U_{r_{ik}}, U_{r_{ik}} = \begin{cases} K_{rep}\left(\frac{1}{d_{ik}} - \frac{1}{D^*}\right) & \text{if } d_{ik} < D^*, \\ 0 & \text{otherwise,} \end{cases} \tag{53}$$

where K_{rep} is a positive gain, D^* is the activation distance for the potential and d_{ik} is the distance between the i-th robot and the k-th obstacle, while Q is the number of total obstacles in the environment.

Without loss of generality, robot 1 has been chosen as the leader of the group and it has been joined to the local device by the PD-like coupling proposed in [11] in order to passively exploit the position of the local robot for driving a mobile robot.

Being the control architecture structured as in Fig.4 and owing to the passivity of the proposed interconnection, the overall system remains passive, as stated in Prop. 5.

The human can transmit the motion of the local device to the leader via the PD-like interconnection and, through the couplings, to the other robots.

Thanks to the PD-like coupling between local and remote sides, the user will receive a feedback informing her/him about the dynamics and the interaction of the leader with all the other coupled robots. See [11] for a more detailed explanation of the kind of feedback that can be achieved using such a coupling.

Being the control architecture structured as in Fig.4 and owing to the passivity of the proposed interconnection, the overall system remains passive, as stated in Prop. 5.

Thus, the overall shared autonomy system is composed of the human, who takes care of driving the fleet towards a desired direction, and of an autonomy allocation unit that shapes the cohesive behavior of the group according to the structure of the environment. The proposed architecture implements at each time the best passive approximation of $\mathbf{F}_C^d$.

The fleet starts from a widespread formation with $\bar{\mathbf{x}}_{12}^d(t) = [-0.75, -0.75, 0]$, $\bar{\mathbf{x}}_{13}^d(t) = [0.75, -0.75, 0]$, $\bar{\mathbf{x}}_{23}^d(t) = [1.5, 0, 0]$ and they are driven towards a narrow bottleneck after which there are no obstacles. The local autonomy module detects the bottleneck and sets each element of $\bar{\mathbf{x}}_{ji}^d(t)$ to a third of its initial value in order to ease the passage. Once the robots traverse the bottleneck, the autonomy allocation unit sets $\bar{\mathbf{x}}_{ji}^d(t)$ back to its initial value. The set of experiments can be seen in the accompanying video.

We initially evaluate the passivity of the group of robots first by directly applying (51) to the robots and then exploiting the proposed architecture. To do so, we evaluate the energy flow through the port $(\mathbf{F}_{R_1}, \mathbf{v}_1)$:

$$\int_0^t \mathbf{F}_{R_1}^T(\tau)\mathbf{v}_1(\tau)d\tau. \tag{54}$$

A negative value of (54) implies a non passive behavior. The evolution of (54) is reported in Fig. 7 and it clearly shows that the variation of $\bar{\mathbf{x}}_{ji}^d(t)$ is a non passive operation and that the proposed architecture allows to restore the passivity.

In the accompanying video, the force produced on the leader by the motion of the local device and the corresponding force feedback provided to the user is shown. The force sent back to the user is given by the dynamic interaction of the leader with the other robots through the passified desired interconnection (51) and by the external forces produced by (52). This kind of feedback provides the user with a, sometimes rough, information about the status of the overall behavior of the multi-robot systems.

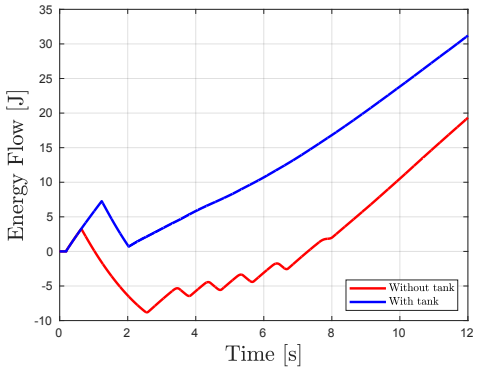

Fig. 7. The energy flow in the system during the experiment, with the proposed architecture (solid blue line) and without using energy tanks (solid red line). In case of direct application, the energy flow becomes negative, meaning that the overall system loses its passivity. When using the proposed architecture, the energy flow is always non negative.

In the following experiment we aim at verifying how the optimization strategy in (25) can guarantee a passive behavior of the group of robots in different situations. We performed the same navigation with variable cohesive behavior using different values of K_P and exploiting the architecture proposed in the paper. The stiffer the coupling, i.e. the larger is K_P, the more dramatic the variation of the rest length $\bar{x}_{ji}^d(t)$ is, i.e. the more energy can be produced.

In Fig. 8 the energy of the tank is portrayed. Using a lower value for $K_P = 20\frac{N}{m}$ the energy in the tank always remains above ε. Thus, according to Prop. 2, the system remains passive at all times and the desired behaviour is perfectly reproduced. The larger value of $K_P = 50\frac{N}{m}$ leads to a higher energy consumption. Nevertheless, once the energy in the tank reaches the imposed lower bound $\varepsilon = 5$, the constraint (28b) stops the extraction process, thus avoiding the tank singularity and preserving the overall passivity, as stated in Prop. 3. This is achieved by implementing the closest passive approximation of the desired control input $\mathbf{F}_C^d$. The difference in the resulting motions can be observed in Fig. 9. In the high stiffness case, it is possible to notice the approximation of the nominal motion.

The last experiments aims at validating the robustness of the proposed architecture with respect to communication delays. We consider the presence of a communication delay δ_{ij} in the exchange of data between robot i and robot j. As presented in Sec.VI, each robot is endowed with a modulated tank and with an authority allocation module. The authority allocation module computes (51) using the local information and the delayed information coming from the other robot, which is passively reproduced by the modulated tank. Additionally, each tank exchanges power with the other tanks following a

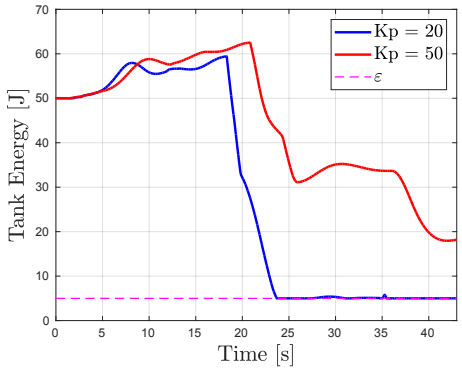

Fig. 8. The energy value of the tank using different values of K_P. Larger values of K_P lead to greater energy extraction. Once the energy in the tank reaches the lower bound ε, the extraction process is halted.

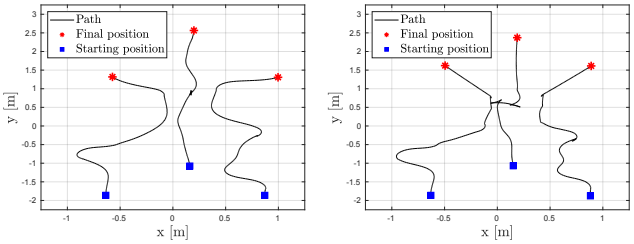

(a) (b)

Fig. 9. Different paths of the formation for (a) $K_P = 20$ and no tank saturation (b) $K_P = 50$ and tank saturation during the second variation of rest length. In the second case, it can be noticed the approximation of the nominal motion, in which the robots are forced to rotate on the spot to maintain the passivity.

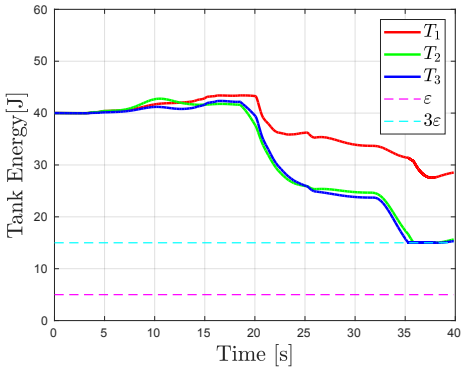

(a) $T_i(0) = 40J$

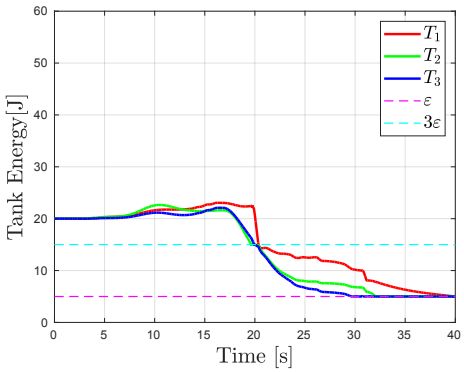

(b) $T_i(0) = 25J$

Fig. 10. Different energy flows in the tanks according to different initial energy values $T_i(0)$. When $T_i(0) = 40J$, the power is equally exchanged among all agents until the values T_2 and T_3 drop below the threshold 3ε. Then they stop sharing their energy and utilize the power coming from T_1. When $T_i(0) = 25J$, this phenomenon is less noticeable, but the energy saturation can be easily observed for T_2 and T_3.

simple power sharing strategy:

$$P_{out_{ij}} = \begin{cases} \overline{P} & \text{if } d_{ij} < D_s \text{ and } T_i \geq 3\varepsilon, \\ 0 & \text{otherwise,} \end{cases} \tag{55}$$

where $\overline{P} = 10W$ is a constant power value, d_{ij} is the distance between the agents and $D_s = 3.5m$ is the maximum sensing range of the robots. Applying this strategy, each robot will exchange power with all the other members of the fleet inside its sensing range, as long as a sufficient surplus of energy is still present in its tank.

The navigation experiment is first run using the distributed tank architecture with the power sharing structure reported in (55) and with $\delta_{ij} = 0$ for all $i, j \in \{1, \dots, 3\}$. The energy in the tanks is reported in Fig. 10.

In Fig. 10a, $T_i(0) = 40J$ for $i = \{1, 2, 3\}$ and the power is equally exchanged among all agents until the values T_2 and T_3 reach the threshold $3\varepsilon = 15J$. After that, they stop sharing their energy with the other tanks and they utilize the power coming from T_1 to compensate the energy extraction due to the rest length variation. In Fig. 10b, in which the tanks are initialized to $25J$, this phenomenon is less evident but T_2 and T_3 reach the threshold $3\varepsilon = 15J$ before T_1 that feeds them for a short interval of time. In the last part of the navigation experiment, tanks do not share energy anymore but they use their own energy to passively complete the task. In fact, it can be noticed that the energy of all the tanks remains above the minimum threshold ε.

Finally, the navigation experiment has been conducted considering a $500ms$ and a $750ms$ delay in the communication among the robots. The evolution of the energy flows is reported in Fig. 11a and Fig. 11b. Here, we also portray the value of H_{ch}, namely the energy stored in the communication channel due to the delay. We can observe how the value of H_{ch} remains constant after a short transient while all the agents equally share power to then lower once the energy in the tanks reaches 3ε, threshold at which the power emission stops. At this point, the energy stored in the channel gradually recharges each tank, compensating the energy loss due to the rest length variation. As proven in Prop. 4, the system remains passive in the presence of the finite delay. Fig. 12 depicts the resulting paths, in which the performance degradation due to the presence of the delay is evident.

B. Comparative Study

In order to show the benefits of the proposed architecture in terms of increased robustness and tracking performance, we conducted an experimental campaign in which we compared the control strategy presented in the paper with state-of-the-art energy tank-based controller.

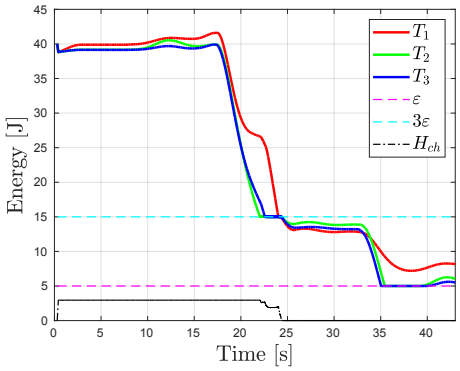

(a) $\delta_{ij} = 500ms$

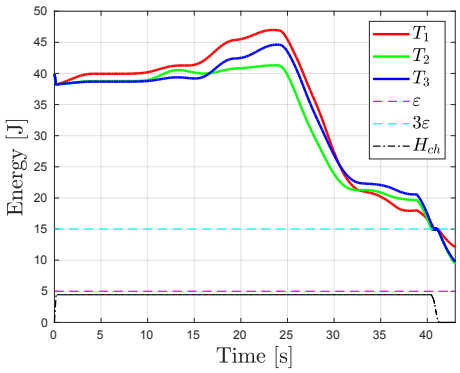

(b) $\delta_{ij} = 750ms$

Fig. 11. Different energy flows in the tanks according to different values of the delay δ_{ij} in the communication channel. The energy stored in the communication channel due to the delay H_{ch} remains constant until the energy in the tanks reaches 3ε. Then, the power emission stops.

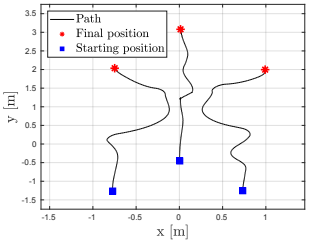

(a) $\delta_{ij} = 500ms$

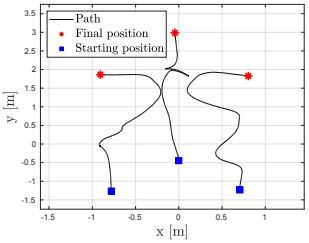

(b) $\delta_{ij} = 750ms$

Fig. 12. Different paths of the formation for different values of the communication delay δ_{ij}. It can be clearly noticed the performance loss due to the presence of the delay.

We recreated the previous multi-robot setup in a simulated environment, in order to maximize the repeatability and reproducibility of the implemented behaviours, thus providing a fair comparison. We then conducted the previous experiments of passive rest length variations, first using our proposed control architecture (without communication delay) and then with a standard energy tank-based controller. The chosen controller makes use of a variable damper for refilling the tank, which is activated as the lower bound ε is reached and more energy is being requested, similarly to [11]. In this way, the overall passivity of the system is guaranteed, but at the cost of introducing extra damping into the dynamics. Thus, following

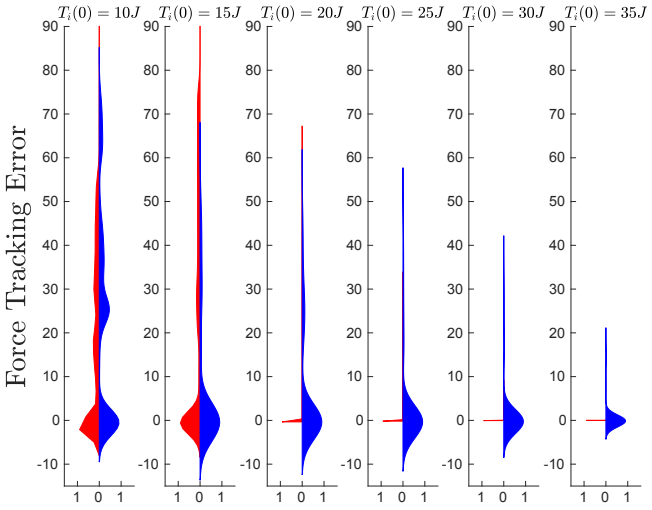

Fig. 13. Violin plots representing the distribution of the force tracking error during the simulations obtained using the presented architecture (in red) and the standard damping injection approach (in blue), for different values of the initial tank energy $T_i(0)$.

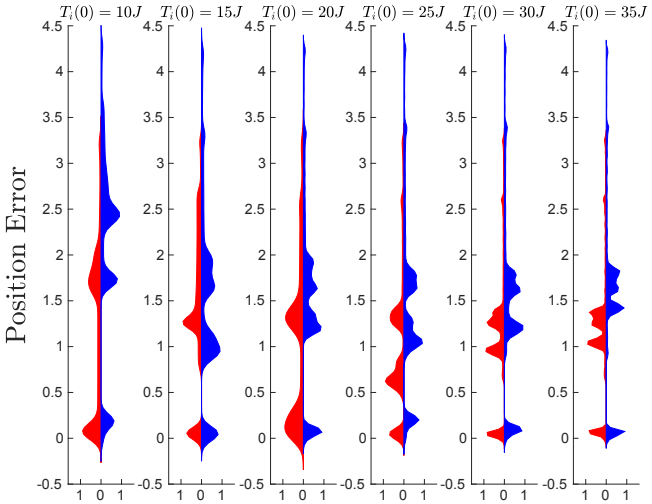

Fig. 14. Violin plots representing the distribution of the pose error during the simulations obtained using the presented architecture (in red) and the standard damping injection approach (in blue), for different values of the initial tank energy $T_i(0)$.

the standard tank-based approach, the power flow through each tank is computed as

$$\dot{T}_i = \dot{\mathbf{x}}_i^T \left(\mathbf{D}_i + (1 - b_i)\, \overline{\mathbf{D}}_i \right) \dot{\mathbf{x}}_i - \dot{\mathbf{x}}_i^T \mathbf{F}_{C_i}^P, \tag{56}$$

where $\overline{\mathbf{D}}_i = \overline{\mathbf{D}}_i(t) \geq 0$ is a positive semi-definite variable damping matrix, while the control input for each robot is computed as

$$\mathbf{F}_{C_i}^P = b_i \mathbf{F}_{C_i}^d \tag{57}$$

and b_i serves to attach or detach the $i-$th tank from the interconnection and inject the additional damping, i.e.

$$b_i = \begin{cases} 0 & \text{if } T_i = \varepsilon \text{ and } \dot{T}_i \leq 0, \\ 1 & \text{otherwise.} \end{cases} \tag{58}$$

The variable damping term $\overline{\mathbf{D}}_i$ is set as a constant diagonal matrix with elements $\bar{d}_i = 0.5\frac{Ns}{m}$.

The series of simulations were conducted varying the initial energy value in the tank at each run, increasing it gradually from $10J$ up until $35J$. As previously stated (see e.g. Fig. 10), this value affects the degree of approximation of the desired behaviour and, consequently, the overall performance.

The results of the study are presented in Fig. 13 and Fig. 14. The violin plot in Fig. 13 showcases the comparison of the force tracking error, computed as $||\mathbf{F}_C^P - \mathbf{F}_C^d||$, using the two controllers. For each simulation, a corresponding density curve portrays the full distribution of the error. The curves obtained with the two different methods thus indicate how often the desired input is approximated and the magnitude of such approximation. It can be observed how, for low values of $T_i(0)$, both approaches necessarily lead to larger tracking errors in order to preserve passivity. Even in these cases, the magnitude of the errors induced by the standard tank-based approach tends to be larger than the one obtained via our control architecture. This is due to the lack of optimization in the standard energy-tank approach, which simply adds a passivating dynamics. As $T_i(0)$ increases and more energy is made available for implementing the behaviour, it is evident how our approach minimally alters the desired input, while the spurious dynamics introduced by the variable damping leads to more frequent and more significant approximations, thus negatively affecting the quality of the allocated autonomy.

In a similar fashion, the plot in Fig. 14 portrays the distribution of the position error over time, computed as $\sum_{i=1}^{3}\sum_{j>i}^{3} ||\mathbf{x}_{ji} - \bar{\mathbf{x}}_{ji}^d(t)||$, using the two controllers. Due to the larger approximation of the control input induced by the standard tank-based approach, the system requires more time to reach the desired formation, thus leading to more significant position errors on average. This larger convergence time might cause dangerous behaviors during the interaction, such as inter-robot crashes or collisions with undetected obstacles in the environment, as well as leading to counter-intuitive behaviours for the human operating the fleet.

Thus, while the standard energy-tank based approach is simpler to implement than the proposed approach, as it does not require to generate the control input via an optimizer, it induces stronger approximations of the desired behaviour, affecting both the performance and the quality of the overall interaction.

C. Admittance Control

A second validation of the architecture was conducted onto a robotic arm implementing an admittance control task. The experimental setup, shown in Fig. 15, includes a Universal Robot 5e manipulator, equipped with a 6-axis force/torque (F/T) sensor and a tool for grasping magnetic objects. The control frequency of both the robot and the sensor is $500Hz$. The human has to teach the robot the pick and place trajectories for moving a set of objects from a picking station (white plate) to the placing station (black plate). The robot has the knowledge of the picking order and the desired pick and place positions but it is not aware of obstacles that could possibly be present in the scene and, thus, of the trajectory to be performed.

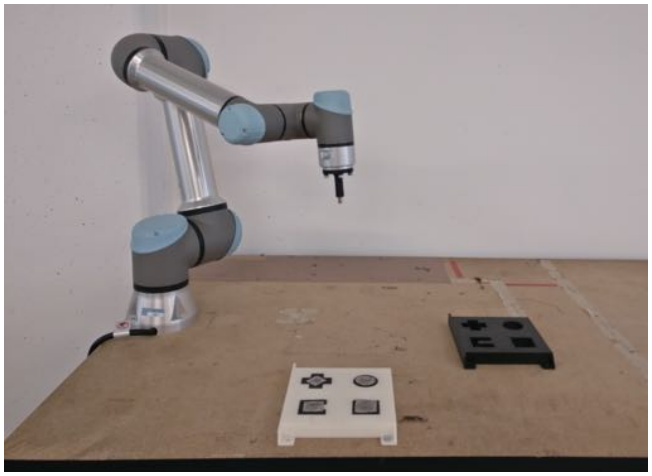

Fig. 15. Experimental setup for the validation considering the admittance control task.

An assisted manual guidance has been implemented through a variable admittance controller using the architecture shown in Sec. VIII. An autonomy allocation unit, given the knowledge of the task and of the environment and the position and velocity of the robot, generates a desired admittance dynamics in the form of a mass-spring-damper system. The inertia and damping matrices chosen for the experiments are diagonal matrices with constant values. In particular, the inertia matrix has elements equal to $1.5kg$ for translations and $1\frac{kg}{m^2}$ for rotations, while the damping matrix has elements equal to $300\frac{Ns}{m}$ and $100\frac{Nms}{rad}$ for translations and rotations respectively.

The stiffness is chosen as a time-varying diagonal matrix, in order to help the human around the pick and place positions. In particular, when the robot end-effector is far from the pick and place positions, the stiffness is set equal to zero. When the distance between the end-effector and the desired pick or place position is lower than $0.25m$, then the stiffness elements becomes equal to $500\frac{N}{m}$ and $30\frac{Nm}{rad}$ for translations and rotations, respectively. When the desired object has been picked up or placed, the stiffness values are set again equal to zero, to ease the human movements between the pick and place plates. Fig. 16 shows the stiffness variation during the task execution (only one translational component is shown, since the others behave accordingly). The resulting force due to the stiffness is then shown in Fig. 17, where the norm of the three translational components is shown.

By integrating the desired time-varying admittance, the corresponding desired velocity $\mathbf{v}_{adm,d}$ can be computed. Since varying online the stiffness of the admittance can lead to a non passive behavior (see e.g. [36]), $\mathbf{v}_{adm,d}$ is sent to the optimizer. The optimizer, considering the energy stored in the tank, computes the best passive approximation $\mathbf{v}_d^P(t)$ of the desired behaviour. The value of $\mathbf{v}_d^P(t)$ is then used for modulating the energy flowing into/out of the tank and, by inverse kinematics, computing the desired joint velocity input for the robot.

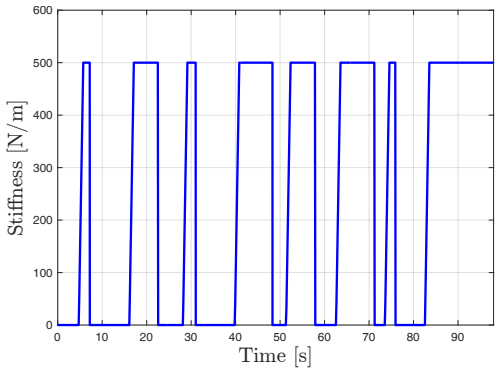

Fig. 16. The evolution over time of the stiffness of the admittance control during the execution of the task.

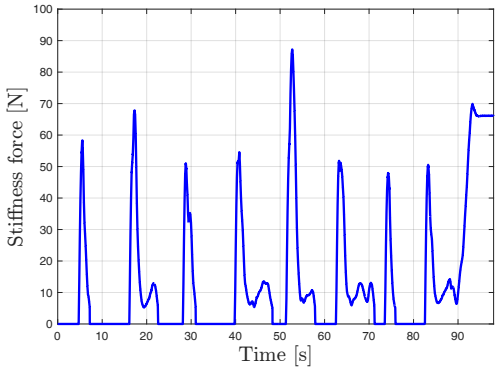

Fig. 17. The evolution over time of the force due to the stiffness application during the execution of the task (norm of the three translational components).

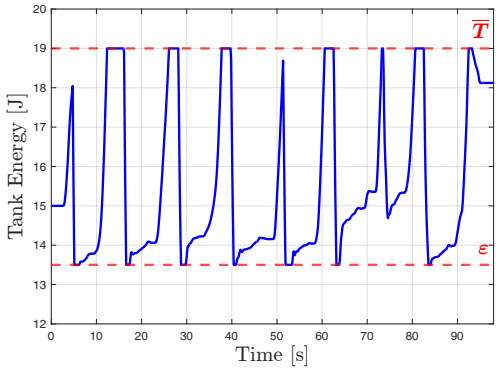

Fig. 18. The evolution over time of the energy in the tank during the execution of the admittance control task.

Fig. 18 shows the evolution of the energy in the tank, which is reminiscent of the previous experiments: as in Fig. 8, once the energy level drops below $\varepsilon = 13.5J$, the constraint (50b) implements the best passive approximation of $\mathbf{v}_{adm,d}$, thus stopping the energy extraction and preserving the overall passivity. An upper bound has been set at $\overline{T} = 19J$ in order to avoid excessive energy storage and for showing the activation of the optimizer.

All of the experiments are portrayed in the accompanying video.

X. Conclusions

In this paper we have proposed a novel energy-based architecture that enables to reproduce the desired autonomy of a robotic system while guaranteeing a robustly stable behavior. Energy tanks have been exploited for enabling a flexible utilization of the energy of the system and for allowing to reproduce dynamic behaviors that could not be implemented using traditional passivity-based control. A convex optimization problem for choosing the closest passive behavior to the desired autonomy has been designed. Experimental results show the effectiveness and the robustness of the proposed control architecture.

References

[1] C. Song, X. Ma, X. Xia, P. Wai Yan Chiu, C. Ching Ning Chong, and Z. Li, "A robotic flexible endoscope with shared autonomy: a study of mockup cholecystectomy," *Surgical Endoscopy*, vol. 34, pp. 2730–2741, 2020.

[2] G. De Rossi, M. Minelli, A. Sozzi, N. Piccinelli, F. Ferraguti, F. Setti, M. Bonfé, C. Secchi, and R. Muradore, "Cognitive robotic architecture for semi-autonomous execution of manipulation tasks in a surgical environment," in *2019 IEEE/RSJ International Conference on Intelligent Robots and Systems (IROS)*, 2019, pp. 7827–7833.

[3] V. Pruks, K. Lee, and J. Ryu, "Shared teleoperation for nuclear plant robotics using interactive virtual guidance generation and shared autonomy approaches," in *2018 15th International Conference on Ubiquitous Robots (UR)*, 2018, pp. 91–95.

[4] M. Ramacciotti, M. Milazzo, F. Leoni, S. Roccella, and C. Stefanini, "A novel shared control algorithm for industrial robots," *Intenational Journal of Advanced Robotic Systems*, vol. 13, no. 6, 2016.

[5] F. Ferraguti, C. Talignani Landi, L. Sabattini, M. Bonfé, C. Fantuzzi, and C. Secchi, "A variable admittance control strategy for stable physical human–robot interaction," *International Journal of Robotics Research*, vol. 38, no. 6, pp. 747–765, May 2019.

[6] F. Ferraguti, R. Villa, C. Talignani Landi, A. Zanchettin, P. Rocco, and C. Secchi, "A unified architecture for physical and ergonomic human–robot collaboration," *Robotica*, vol. 38, no. 4, p. 669–683, 2020.

[7] A. Ajoudani, P. Albrecht, M. Bianchi, A. Cherubini, S. Del Ferraro, P. Fraisse, L. Fritzsche, M. Garabini, A. Ranavolo, P. H. Rosen, M. Sartori, N. Tsagarakis, B. Vanderborght, and S. Wischniewski, "Smart collaborative systems for enabling flexible and ergonomic work practices [industry activities]," *IEEE Robotics Automation Magazine*, vol. 27, no. 2, pp. 169–176, 2020.

[8] C. T. Landi, V. Villani, F. Ferraguti, L. Sabattini, C. Secchi, and C. Fantuzzi, "Relieving operators' workload: Towards affective robotics in industrial scenarios," *Mechatronics*, vol. 54, pp. 144 – 154, 2018.

[9] Y. Li, K. P. Tee, W. L. Chan, R. Yan, Y. Chua, and D. K. Limbu, "Continuous role adaptation for human–robot shared control," *IEEE Transactions on Robotics*, vol. 31, no. 3, pp. 672–681, 2015.

[10] Y. Yang, D. Constantinescu, and Y. Shi, "Connectivity-preserving swarm teleoperation with a tree network," in *2019 IEEE/RSJ International Conference on Intelligent Robots and Systems (IROS)*, 2019, pp. 3624–3629.

[11] A. Franchi, C. Secchi, H. I. Son, H. H. Bulthoff, and P. R. Giordano, "Bilateral teleoperation of groups of mobile robots with time-varying topology," *IEEE Transactions on Robotics*, vol. 28, no. 5, pp. 1019–1033, Oct 2012.

[12] E. J. Rodríguez-Seda, J. J. Troy, C. A. Erignac, P. Murray, D. M. Stipanovic, and M. W. Spong, "Bilateral teleoperation of multiple mobile agents: Coordinated motion and collision avoidance," *IEEE Transactions on Control Systems Technology*, vol. 18, no. 4, pp. 984–992, 2010.

[13] M. Selvaggio, M. Cognetti, S. Nikolaidis, S. Ivaldi, and B. Siciliano, "Autonomy in physical human-robot interaction: A brief survey," *IEEE Robotics and Automation Letters*, vol. 6, no. 4, pp. 7989–7996, 2021.

[14] B. Hayes and J. A. Shah, "Improving robot controller transparency through autonomous policy explanation," in *2017 12th ACM/IEEE International Conference on Human-Robot Interaction (HRI*, 2017, pp. 303–312.

[15] H. Liu, T. Fang, T. Zhou, and L. Wang, "Towards robust human-robot collaborative manufacturing: Multimodal fusion," *IEEE Access*, vol. 6, pp. 74 762–74 771, 2018.

[16] A. Broad, I. Abraham, T. Murphey, and B. Argall, "Data-driven koopman operators for model-based shared control of human–machine systems," *The International Journal of Robotics Research*, vol. 29, no. 9, 2020.

[17] M. Ohnishi, L. Wang, G. Notomista, and M. Egerstedt, "Barrier-certified adaptive reinforcement learning with applications to brushbot navigation," *IEEE Transactions on Robotics*, vol. 35, no. 5, pp. 1186–1205, 2019.

[18] Y. Yang, Y. Yin, W. He, K. G. Vamvoudakis, H. Modares, and D. C. Wunsch, "Safety-aware reinforcement learning framework with an actor-critic-barrier structure," in *2019 American Control Conference (ACC)*, 2019, pp. 2352–2358.

[19] C. D. McKinnon and A. P. Schoellig, "Learn fast, forget slow: Safe predictive learning control for systems with unknown and changing dynamics performing repetitive tasks," *IEEE Robotics and Automation Letters*, vol. 4, no. 2, pp. 2180–2187, 2019.

[20] L. Villani and J. De Schutter, "Force control," in *Handbook of Robotics*. Springer, 2016, pp. 195–220.

[21] G. Niemeyer and J. J. E. Slotine, "Stable adaptive teleoperation," *IEEE Journal of Oceanic Engineering*, vol. 16, no. 1, pp. 152–162, Jan 1991.

[22] N. E. Leonard and E. Fiorelli, "Virtual leaders, artificial potentials and coordinated control of groups," in *Proceedings of the 40th IEEE Conference on Decision and Control (Cat. No.01CH37228)*, vol. 3, 2001, pp. 2968–2973 vol.3.

[23] C. Secchi, S. Stramigioli, and C. Fantuzzi, *Control of Interactive Robotic Interfaces: a port-Hamiltonian Approach*. Springer, 2007.

[24] S. Stramigioli, "Energy aware robotics," in *Mathematical Control Theory I*, C. J. J. A. P. R. S. J. (eds), Ed. Springer, 2015, pp. 37–50.

[25] E. Nuno, R. Ortega, N. Barabanov, and L. Basanez, "A globally stable pd controller for bilateral teleoperators," *IEEE Transactions on Robotics*, vol. 24, no. 3, pp. 753–758, 2008.

[26] F. Ferraguti, M. Bonfe, C. Fantuzzi, and C. Secchi, "Optimized power modulation in wave based bilateral teleoperation," *IEEE/ASME Transactions on Mechatronics*, pp. 1–1, 2020.

[27] L. Sabattini, C. Secchi, B. Capelli, and C. Fantuzzi, "Passivity preserving force scaling for enhanced teleoperation of multirobot systems," *IEEE Robotics and Automation Letters*, vol. 3, no. 3, pp. 1925–1932, 2018.

[28] M. Angerer, S. Music, and S. Hirche, "Port-hamiltonian based control for human-robot team interaction," in *2017 IEEE International Conference on Robotics and Automation (ICRA)*, May 2017, pp. 2292–2299.

[29] T. Zhang and J. Xia, "Interconnection and damping assignment passivity-based impedance control of a compliant assistive robot for physical human–robot interactions," *IEEE Robotics and Automation Letters*, vol. 4, no. 2, pp. 538–545, 2019.

[30] C. Yang, G. Ganesh, S. Haddadin, S. Parusel, A. Albu-Schäffer, and E. Burdet, "Human-like adaptation of force and impedance in stable and unstable interactions." *IEEE Transactions on Robotics*, vol. 27, no. 5, pp. 918–930, 2011.

[31] F. Dimeas and N. Aspragathos, "Online stability in human-robot cooperation with admittance control," *IEEE Transactions on Haptics*, vol. 9, no. 2, pp. 267–278, 2016.

[32] P. Capsi-Morales, C. Piazza, M. G. Catalano, A. Bicchi, and G. Grioli, "Exploring stiffness modulation in prosthetic hands and its perceived function in manipulation and social interaction," *Frontiers in Neurorobotics*, vol. 14, p. 33, 2020.

[33] M. T. J. Spaan, T. S. Veiga, and P. U. Lima, "Active cooperative perception in network robot systems using pomdps," in *2010 IEEE/RSJ International Conference on Intelligent Robots and Systems*, Oct 2010, pp. 4800–4805.

[34] M. Schwager, M. P. Vitus, S. Powers, D. Rus, and C. J. Tomlin, "Robust adaptive coverage control for robotic sensor networks," *IEEE Transactions on Control of Network Systems*, vol. 4, no. 3, pp. 462–476, Sept 2017.

[35] M. Franken, S. Stramigioli, S. Misra, C. Secchi, and A. Macchelli, "Bilateral telemanipulation with time delays: A two-layer approach combining passivity and transparency." *IEEE Transactions on Robotics*, vol. 27, no. 4, pp. 741–756, 2011.

[36] F. Ferraguti, N. Preda, A. Manurung, M. Bonfè, O. Lambercy, R. Gassert, R. Muradore, P. Fiorini, and C. Secchi, "An energy tank-based interactive control architecture for autonomous and teleoperated robotic surgery," *IEEE Transactions on Robotics*, vol. 31, no. 5, pp. 1073–1088, Oct 2015.

[37] G. Riggio, C. Fantuzzi, and C. Secchi, "On the use of energy tanks for multi-robot interconnection," in *2018 IEEE/RSJ International Conference on Intelligent Robots and Systems (IROS)*, 2018, pp. 3738–3743.

[38] C. Secchi and F. Ferraguti, "Energy optimization for a robust and flexible interaction control," in *2019 International Conference on Robotics and Automation (ICRA)*, 2019, pp. 1919–1925.

[39] P. Abbott, J.J.and Marayong and A. Okamura, "Haptic virtual fixtures for robot-assisted manipulation," in *Robotics Research*, ser. Springer Tracts in Advanced Robotics, D.-W. H. e. Thrun S., Brooks R., Ed. Springer, 2007, vol. 28, pp. 49–64.

[40] J. Ren, R. V. Patel, K. A. McIsaac, G. Guiraudon, and T. M. Peters, "Dynamic 3-d virtual fixtures for minimally invasive beating heart procedures," *IEEE Transactions on Medical Imaging*, vol. 27, no. 8, pp. 1061–1070, 2008.

[41] D. Powell and M. K. O'Malley, "The task-dependent efficacy of shared-control haptic guidance paradigms," *IEEE Transactions on Haptics*, vol. 5, no. 3, pp. 208–219, 2012.

[42] A. W. de Jonge, J. G. W. Wildenbeest, H. Boessenkool, and D. A. Abbink, "The effect of trial-by-trial adaptation on conflicts in haptic shared control for free-air teleoperation tasks," *IEEE Transactions on Haptics*, vol. 9, no. 1, pp. 111–120, 2016.

[43] H. Su, X. Wang, and Z. Lin, "Flocking of multi-agents with a virtual leader," *IEEE Transactions on Automatic Control*, vol. 54, no. 2, pp. 293–307, 2009.

[44] A. Tahirovic and G. Magnani, "General framework for mobile robot navigation using passivity-based mpc," *IEEE Transactions on Automatic Control*, vol. 56, no. 1, pp. 184–190, 2011.

[45] B. Henze, M. A. Roa, and C. Ott, "Passivity-based whole-body balancing for torque-controlled humanoid robots in multi-contact scenarios," *The International Journal of Robotics Research*, vol. 35, no. 12, pp. 1522–1543, 2016. [Online]. Available: https://doi.org/10.1177/0278364916653815

[46] M. Sharf and D. Zelazo, "Network feedback passivation of passivity-short multi-agent systems," *IEEE Control Systems Letters*, vol. 3, no. 3, pp. 607–612, 2019.

[47] B. Hannaford and Jee-Hwan Ryu, "Time-domain passivity control of haptic interfaces," *IEEE Transactions on Robotics and Automation*, vol. 18, no. 1, pp. 1–10, 2002.

[48] M. Panzirsch, J. Artigas, A. Tobergte, P. Kotyczka, C. Preusche, A. Albu-Schaeffer, and G. Hirzinger, "A peer-to-peer trilateral passivity control for delayed collaborative teleoperation," in *Haptics: Perception, Devices, Mobility, and Communication*, P. Isokoski and J. Springare, Eds. Berlin, Heidelberg: Springer Berlin Heidelberg, 2012, pp. 395–406.

[49] R. Balachandran, H. Mishra, M. Cappelli, B. Weber, C. Secchi, C. Ott, and A. Albu-Schaeffer, "Adaptive authority allocation in shared control of robots using bayesian filters," in *2020 IEEE International Conference on Robotics and Automation (ICRA)*, 2020, pp. 11 298–11 304.

[50] D. Lee and K. Huang, "Passive-set-position-modulation framework for interactive robotic systems," *IEEE Transactions on Robotics*, vol. 26, no. 2, pp. 354–369, 2010.

[51] D. Lee, A. Franchi, H. I. Son, C. Ha, H. H. Bülthoff, and P. R. Giordano, "Semiautonomous haptic teleoperation control architecture of multiple unmanned aerial vehicles," *IEEE/ASME Transactions on Mechatronics*, vol. 18, no. 4, pp. 1334–1345, 2013.

[52] D. Heck, A. Saccon, R. Beerens, and H. Nijmeijer, "Direct force-reflecting two-layer approach for passive bilateral teleoperation with time delays," *IEEE Transactions on Robotics*, vol. 34, no. 1, pp. 194–206, Feb 2018.

[53] M. Selvaggio, P. Robuffo Giordano, F. Ficuciellol, and B. Siciliano, "Passive task-prioritized shared-control teleoperation with haptic guidance," in *2019 International Conference on Robotics and Automation (ICRA)*, 2019, pp. 430–436.

[54] C. Schindlbeck and S. Haddadin, "Unified passivity-based cartesian force/impedance control for rigid and flexible joint robots via task-energy tanks," in *2015 IEEE International Conference on Robotics and Automation (ICRA)*, 2015, pp. 440–447.

[55] E. Shahriari, L. Johannsmeier, E. Jensen, and S. Haddadin, "Power flow regulation, adaptation, and learning for intrinsically robust virtual energy tanks," *IEEE Robotics and Automation Letters*, vol. 5, no. 1, pp. 211–218, 2020.

[56] E. Shahriari, A. Kramberger, A. Gams, A. Ude, and S. Haddadin, "Adapting to contacts: Energy tanks and task energy for passivity-based dynamic movement primitives," in *2017 IEEE-RAS 17th International Conference on Humanoid Robotics (Humanoids)*, Nov 2017, pp. 136–142.

[57] A. Dietrich, C. Ott, and S. Stramigioli, "Passivation of projection-based null space compliance control via energy tanks," *IEEE Robotics and Automation Letters*, vol. 1, no. 1, pp. 184–191, Jan 2016.

[58] M. Selvaggio, G. A. Fontanelli, F. Ficuciello, L. Villani, and B. Siciliano, "Passive virtual fixtures adaptation in minimally invasive robotic surgery," *IEEE Robotics and Automation Letters*, vol. 3, no. 4, pp. 3129–3136, 2018.

[59] C. Talignani Landi, F. Ferraguti, C. Secchi, and C. Fantuzzi, "A passivity-based strategy for manual corrections in human-robot coaching," *Electronics*, vol. 8, no. 3, pp. 1–16, March 2019.
[60] K. Kronander and A. Billard, "Stability considerations for variable impedance control," *IEEE Transactions on Robotics*, vol. 32, no. 5, pp. 1298–1305, 2016.
[61] T. Kastritsi, F. Dimeas, and Z. Doulgeri, "Progressive automation with dmp synchronization and variable stiffness control," *IEEE Robotics and Automation Letters*, vol. 3, no. 4, pp. 3789–3796, 2018.
[62] G. Notomista and X. Cai, "A safety and passivity filter for robot teleoperation systems," in *International Workshop on Human-Friendly Robotics*. Springer, 2021, pp. 101–115.
[63] R. Ortega, J. Loría Perez, J. Nicklasson, and H. Sira-Ramirez, *Passivity-based Control of Euler-Lagrange Systems*, ser. Communications and Control Engineering. Springer, 1998.
[64] A. van der Schaft, *L2-Gain and Passivity Techniques in Nonlinear Control*, ser. Communications and Control Engineering. Springer, 2016.
[65] L. Sabattini, B. Capelli, C. Fantuzzi, and C. Secchi, "Teleoperation of multi-robot systems to relax topological constraints," in *Proceedings of the IEEE International Conference on Robotics and Automation (ICRA)*, June 2020.
[66] P. R. Giordano, A. Franchi, C. Secchi, and H. Buelthoff, "A passivity-based decentralized strategy for generalized connectivity maintenance," *International Journal of Robotics Research*, vol. 32, no. 3, pp. 299–323, 2013.
[67] G. Raiola, C. A. Cardenas, T. S. Tadele, T. de Vries, and S. Stramigioli, "Development of a safety- and energy-aware impedance controller for collaborative robots," *IEEE Robotics and Automation Letters*, vol. 3, no. 2, pp. 1237–1244, 2018.
[68] J. Mattingley and S. Boyd, "Cvxgen: a code generator for embedded convex optimization," *Optim Eng*, vol. 6, pp. 1–27, 2012.
[69] S. Stramigioli, C. Secchi, A. J. van der Schaft, and C. Fantuzzi, "Sampled data systems passivity and discrete port-hamiltonian systems," *IEEE Transactions on Robotics*, vol. 21, no. 4, pp. 574–587, 2005.
[70] M. De Stefano, R. Balachandran, and C. Secchi, "A passivity-based approach for simulating satellite dynamics with robots: Discrete-time integration and time-delay compensation," *IEEE Transactions on Robotics*, vol. 36, no. 1, pp. 189–203, 2020.
[71] M. Minelli, F. Ferraguti, N. Piccinelli, R. Muradore, and C. Secchi, "An energy-shared two-layer approach for multi-master-multi-slave bilateral teleoperation systems," in *2019 International Conference on Robotics and Automation (ICRA)*, May 2019, pp. 423–429.
[72] G. Niemeyer, C. Preusche, S. Stramigioli, and D. Lee, "Telerobotics," in *Handbook of Robotics*. Springer, 2016, pp. 1085–1108.
[73] W. Zou, P. Duan, Y. Chen, N. Yu, and L. Shi, "Variable stiffness control with strict frequency domain constraints for physical human-robot interaction," in *Proceedings of the IEEE/RSJ International Conference on Intelligent Robots and Systems (IROS)*, Virtual, October 2020, pp. 7146–7151.

Federico Benzi is currently a Ph.D. student in Industrial Innovation Engineering at the University of Modena and Reggio Emilia, Italy. He received the B.Sc. and M.Sc. in Mechatronic Engineering from the University of Modena and Reggio Emilia (Italy) in 2016 and 2019 respectively. He has been a Visiting Researcher at the Autonomous Systems Lab at ETH Zurich, Switzerland in 2021. His main research interests are in the fields of Physical Human-Robot Interaction and Collaborative Robotics.

Federica Ferraguti is currently Assistant Professor at the Department of Sciences and Methods for Engineering, University of Modena and Reggio Emilia, Italy. She received the B.Sc. and M.Sc. in Industrial and Management Engineering from the University of Modena and Reggio Emilia (Italy) in 2008 and 2011 respectively, and her Ph.D. in Industrial Innovation Engineering from the University of Modena and Reggio Emilia (Italy) in 2015. She has been a Visiting Researcher at the Rehabilitation Engineering Lab at ETH Zurich, Switzerland in 2013. Her research deals with collaborative robotics, industrial robotics, augmented reality, surgical robotics, teleoperation, control of robotic systems, physical human-robot interaction and learning from demonstration. She obtained the "Fabrizio Flacco Young Author Best Paper Award 2017" of the IEEE Robotics and Automation Society – Italian Chapter.

Giuseppe Riggio is currently R&D SW Engineer at System Logistics S.p.a., Italy . He received the B.Sc. and M.Sc. in Mechatronic Engineering from the University of Modena and Reggio Emilia (Italy) in 2013 and 2016 respectively, and his Ph.D. in Industrial Innovation Engineering from the University of Modena and Reggio Emilia (Italy) in 2020. His interests include Industrial Robotics and Control of AGVs (Autonomous Guided Vehicles).

Cristian Secchi is a Full Professor of Robotics at the University of Modena and Reggio Emilia. He received his M.Sc. in Computer Engineering from the University of Bologna in 2000 and his Ph.D in Information Engineering from the University of Modena and Reggio Emilia in 2004. In 2006 his thesis on interactive robotic interfaces has been selected as one of the three finalists for the Euron Georges Giralt PhD Award for the best PhD thesis on robotics in Europe. He was a finalist for the 2010 EUROP/EURON Technology Transfer Award for the best Technology transfer project in Europe in the CROW project, He has served as an Associate Editor of the Robotics and Automation Magazine (2005-2008), for the IEEE Transactions on Robotics (2012-2017) and for the IEEE Robotics and Automation Letters (2015-2017). He is leading the research in robotics at the ARSControl lab of the University of Modena and Reggio Emilia. His main research interests are in the fields of human-robot collaboration and of medical robotics.